

**High cell density methanol cultivation  
of *Methylosinus trichosporium OB3b***

by

Olufemi Adegbola

A thesis submitted to the Department of Chemical Engineering

In conformity with the requirements for  
the degree of Master of Science (Engineering)

Queen's University

Kingston, Ontario, Canada

(August, 2008)

Copyright © Olufemi Adegbola, 2008

## Abstract

*Methylosinus trichosporium OB3b* is a wild type, obligate methanotroph that grows only on one-carbon compounds and, in the absence of copper, produces high levels of soluble methane monooxygenase (sMMO) to metabolize methane to methanol. sMMO has gained a great deal of attention in the bioremediation and chemical industries because of its low substrate specificity and its ability to oxidize chlorinated hydrocarbons. Much literature exists on cultivating this organism on methane, however no one has achieved dry cell weight densities exceeding 18 g/L. Biomass growth is limited due to mass transfer of methane to cells. This study investigated the growth of *M. trichosporium* on the water soluble carbon source, methanol while retaining sMMO activity.

Methanol was found to completely inhibit growth at 40 g/L. For online methanol measurements during fed-batch cultivation, an *in situ* probe was constructed from autoclavable materials and equipped with a Figaro TGS822 vapor sensor. The probe was designed to prevent the sensor coming in contact with water aerosols which affect its performance. The probe was an essential component of a feedback methanol control system. The cumulative CO<sub>2</sub> production (CCP) strategy was used to feed methanol in fed-batch experiments.

In an initial bioreactor study, growth nutrients were fed in excess. The yields of biomass to nutrients were determined and the growth medium modified accordingly. A biomass density of 19 g/L (growth rate of 0.013-0.065 h<sup>-1</sup>) was achieved with sMMO activity of 300 to 500 [μmol naphthalol][g of biomass]<sup>-1</sup>[h]<sup>-1</sup>. The subsequent bioreactor

study involved feeding of nutrients based on their yields in relation to methanol, a biomass density of 62 g/L (growth rate of 0.034- 0.08 h<sup>-1</sup>) was achieved.

The inoculum cultures utilized in the bioreactor studies were maintained on Noble agar plates containing nitrogen minimal salts medium and methane. After 6 months of subsequent plate transfers, *M. trichosporium* lost the ability to produce high levels of sMMO. The enzyme activity in methanol grown cells was recovered by subculturing in liquid NMS medium with methane as the sole carbon source, the activity increased from 8 to 600 [ $\mu\text{mol naphthol}$ ][g of biomass]<sup>-1</sup>[h]<sup>-1</sup>. It is recommended that further studies be carried out on stimulating sMMO activity during cultivation on methanol.

## **Acknowledgements**

I would like to extend my sincerest gratitude to my supervisors Dr. Bruce and Juliana Ramsay for their continued guidance and criticism on this project.

I would also like to thank Yinghao Yu and Zhiyong Sun for their help with getting me acquainted with all the laboratory equipment, as well as my other colleagues Paul Phillippe, Bohzi Sun, Jade Jiang, Selvia Soegiaman and Heather Mclean for their feedback and making my lab experience a memorable one.

My appreciation to Ed Maracle, for his technical guidance with setting up the Figaro sensor and making sure the circuitry was in compliance with Canadian regulations as well as for providing his expertise in repairing electronic malfunctions with laboratory equipment.

Furthermore, my thanks to Queen's University for the Queen's Entrance and Graduate student awards for financial aid.

Finally to Lexi, my parents, siblings, loved ones and friends for their support, encouragement and most importantly for understanding the time commitment involved with this project.

## Table of Contents

Abstract.....	ii
Acknowledgements.....	iv
Table of Contents.....	v
List of Figures.....	vii
List of Tables .....	viii
List of Abbreviations .....	ix
Chapter 1 Introduction.....	1
Chapter 2 Literature Review.....	4
2.1 Methanotrophic bacteria .....	4
2.2 Carbon source for cultivating <i>M. trichosporium OB3b</i> .....	5
2.2.1 Methane metabolism.....	6
2.2.2 Methanol metabolism.....	6
2.2.3 Formaldehyde assimilation (serine pathway) .....	8
2.3 Effect of other nutrients on growth .....	8
2.3.1 Effect of nitrogen source.....	8
2.3.2 Effect of phosphate .....	11
2.3.3 Effect of supplemental CO <sub>2</sub> on lag phase .....	11
2.3.4 Effect of metal ions and trace nutrients on growth .....	12
2.4 Soluble methane monooxygenase .....	13
2.4.1 Enzyme structure .....	13
2.4.2 Known inhibitors of sMMO.....	15
Chapter 3 Online methanol measurement.....	17
3.1 Materials and methods .....	18
3.1.1 Online methanol control .....	18
3.1.2 Experimental set-up .....	18
3.1.3 Online methanol detection .....	20
3.1.4 Offline methanol verification.....	21
3.1.5 Sensor characterization .....	21
3.1.6 Sensor performance .....	22
3.2 Results and discussion .....	23
3.2.1 Sensor characterization .....	23
3.2.2 Sensor performance .....	26

3.3 Conclusions.....	28
Chapter 4 High cell density cultivation of <i>Methylosinus trichosporium OB3b</i> on methanol .....	29
4.1 Materials and methods .....	29
4.1.1 Culture maintenance .....	29
4.1.2 Analytical methods .....	30
4.1.3 Shake flask studies: medium optimization.....	34
4.1.4 Bioreactor studies.....	36
4.1.5 Methanol feeding strategy for fed-batch bioreactor cultivation.....	38
4.2 Results and discussion .....	40
4.2.1 Shake flask studies: medium optimization.....	40
4.2.2 Bioreactor studies: medium optimization .....	44
4.2.3 High cell density fed-batch cultivation (Fermentation 2) .....	47
4.3 Conclusions.....	54
Chapter 5 Recovering sMMO activity .....	55
5.1 Materials and methods .....	55
5.2 Results and discussion .....	56
5.2.1 Effect of nitrogen source on sMMO activity .....	56
5.2.2 Effect of allylthiourea on sMMO recovery .....	57
5.2.3 Effect of methane on sMMO activity of methanol grown cells.....	59
5.3 Conclusions.....	61
Chapter 6 Conclusions .....	62
Chapter 7 Recommendations and future work.....	64
Bibliography .....	65
Appendix A Figaro Sensor.....	71
Appendix B Calibration curves.....	72
Appendix C Concentration profile of growth nutrients in Fermentation 1 .....	73
Appendix D Method for estimating specific growth rate in Fed-batch studies .....	79
Appendix E Biomass yield estimation.....	81

## List of Figures

Figure 2-1: Oxidation of methane to formaldehyde.....	7
Figure 2-2: Serine pathway for the assimilation of formaldehyde.....	7
Figure 2-3: Hypothetical structure of the active-site of MMOH. ....	14
Figure 3-1: Methanol control system. ....	19
Figure 3-2: Response time of sensor to a step change in methanol .....	24
Figure 3-3: Sensitivity to airflow rate through probe .....	24
Figure 3-4: Sensor performance during fermentation. ....	27
Figure 4-1: Methanol feeding strategy.....	39
Figure 4-2: Fail safe methanol control.....	39
Figure 4-3: Inhibitory effect of methanol on growth.....	41
Figure 4-4: Inhibitory effect of ammonium on growth.....	41
Figure 4-5: Fermentation 1: Biomass, methanol, CCP , CMC and $Y_{CO_2/CH_3OH}$ profiles. ....	45
Figure 4-6: Trace nutrients feeding strategy.....	48
Figure 4-7: Fermentation 2: Biomass, methanol, $Y_{CO_2/CH_3OH}$ , CCP and CMC profiles.....	51
Figure 4-8: Ammonium and phosphate concentration profiles.....	53
Figure 4-9: Fermentation 2: Effect of ammonium on growth rate.....	53
Figure 5-1: Recovery of sMMO activity in subcultures grown on methane.....	60

## List of Tables

Table 1-1: Maximum degradation rates by TCE-degraders.....	2
Table 2-1: Characteristics of Methanotrophs.....	5
Table 2-2: Effect of medium components on <i>M. trichosporium OB3b</i> .....	16
Table 4-1: Composition of the four culture media used in this study .....	30
Table 4-2: Summary of operating conditions of two fed-batch fermentation experiments .....	37
Table 4-3: Effect of antifoam Sigma 204 on methanol and ammonium uptake .....	42
Table 4-4: Effect of different antifoams on methanol and ammonium uptake .....	43
Table 4-5: Fermentation 1: Growth and sMMO production summary .....	46
Table 4-6: Biomass yields of <i>Methylosinus trichosporium OB3b</i> on nutrients .....	46
Table 4-7: Concentrated trace nutrient feed solution.....	48
Table 4-8: Fermentation 2: Growth and sMMO production summary .....	50
Table 5-1: Effect of equimolar concentration of ammonium and nitrate on sMMO activity .....	57
Table 5-2: Effect of allylthiourea on methanol and methane grown cells .....	58

## List of Abbreviations

ATP	Adenosine triphosphate
CCP	Cumulative carbon dioxide production
CMC	Cumulative methanol consumption
DO	Dissolved oxygen
GC	Gas chromatography
NADH	Nicotinamide adenine dinucleotide –reduced
NAD(P)H	Nicotinamide adenine dinucleotide phosphate –reduced
NMS	Nitrogen minimal salts medium
MDH	Methanol dehydrogenase
MMO	Methane monooxygenase
MMOH	Hydroxylase component of sMMO enzyme
RuMP	Ribulose monophosphate pathway
pMMO	Particulate methane monooxygenase
sMMO	Soluble methane monooxygenase
STHM	Serine hydroxymethyltransferease
TCA	Tricarboxylic acid
TCE	Trichloroethylene

## **Chapter 1**

### **Introduction**

*Methylosinus trichosporium* is a Gram-negative bacterium that occurs naturally in aquatic and terrestrial environments. It is an  $\alpha$ -proteobacterium in the family *Methylocystaceae* that is representative of all Type II methanotrophs. Methanotrophs utilize one-carbon compounds as a source of carbon and energy. Type II methanotrophs can co-metabolize a broad range of substrates due to their synthesis of soluble methane monooxygenase (sMMO) which catalyzes the breakdown of methane to methanol. There are two types of methane monooxygenase (MMO), the particulate form (pMMO) and the soluble form (sMMO). The soluble form has been shown to possess a broader range of substrate specificity (Colby, et al., 1977; Hanson and Hanson, 1996), resulting in faster degradation rates of chlorinated ethenes than the particulate form (DiSpirito et al., 1991; Oldenhuis et al., 1991).

Due to its low substrate specificity, sMMO has been studied for use in the bioremediation industry for the degradation of a host of contaminants including naphthalene (Cardinal and Stenstrom, 1991), trichloroethylene (Brusseau et al., 1990; Tsien et al., 1989), dichloroethane (Oldenhuis et al., 1989), vinyl chloride (Fox et al., 1990) and cyclopropane (Dalton et al., 1981). For instance, the degradation of trichloroethylene, a recalcitrant carcinogenic groundwater contaminant (Canadian Council of Ministers of the Environment 2006), is facilitated by sMMO via an epoxidation reaction. The enzyme can also be used in the production of commercially significant epoxides such as propylene oxide (Lidstrom and Stirling, 1990). Degradation

rates of TCE by sMMO expressing cultures of *M. trichosporium* OB3b have been reported to be up to three orders of magnitude faster than those observed in other TCE degraders (Table 1-1).

**Table 1-1: Maximum degradation rates by TCE-degraders (Suarez and Rifai, 1999)**

Type of study	Redox Environment	Culture	Max. specific degradation rate (mg/mg-day)	Initial concentration (mg/L)	Reference
Growth reactor	aerobic - co-metabolism (methane)	mixed methanotrophs	0 - 1.13	1.00	Anderson and McCarty, 1996
Growth reactor	aerobic - co-metabolism (phenol)	filamentous phenol-oxidizers	0.10 - 0.25		Bielefeldt et al., 1994
Growth reactor	aerobic - co-metabolism (propane)	propane oxidizing culture	0.04	3	Keenan et al., 1994
Continuous reactor	aerobic - co-metabolism (methane)	sMMO expressing <i>Methylosinus trichosporium</i> OB3b	54.71	9.17 -13.10	Oldenhuis et al., 1991

*M. trichosporium* OB3b is a wild type that has been shown to produce high levels of sMMO in comparison to other sMMO producers (Bowman and Sayler, 1994). Since sMMO is a growth associated enzyme, high cell density cultivation of *M. trichosporium* OB3b could result in increased enzyme production. An advantage of high cell densities is faster contaminant degradation. A major problem encountered in high cell density cultivation of this organism, is the solubility of methane in liquid medium. At high cell

densities, the availability of the carbon source is primarily limited by mass transfer of gaseous methane to the aqueous phase. A potential solution to this problem is the use of a water soluble carbon source. Methanol although it inhibits growth above certain concentrations, is a good alternative due to its infinite solubility in water, and low cost. In addition, methanol is less flammable than methane and thus has less of a hazard for large scale use.

This study investigates the cultivation of *M. trichosporium OB3b* on methanol to achieve high biomass concentrations whilst retaining sMMO activity.

## **Chapter 2**

### **Literature Review**

This chapter provides a summary of scholarly articles concerning the cultivation of *M. trichosporium OB3b* and the expression of sMMO.

#### **2.1 Methanotrophic bacteria**

*M. trichosporium* is an aerobic, obligate methanotroph that can only utilize C1- carbon sources such as methane and methanol as primary growth substrates. It is a Type II methanotroph producing both soluble (sMMO) and particulate (pMMO) forms of methane monooxygenase. The sMMO is produced in the cell cytoplasm only under copper limited conditions, while pMMO which is associated with membranes, is preferentially expressed in copper sufficient medium. Copper concentrations as low as 0.25  $\mu\text{M}$  were shown to suppress sMMO production in *M. trichosporium OB3b* (Brusseau et al., 1990). Type I methanotrophs produce only the particulate form of the enzyme. Type X methanotrophs possess certain properties in common with both Type I and II. A summary of the major differences between methanotrophs is shown in Table 2-1 (Hanson and Hanson, 1996). Methane is the most widely used substrate employed in cultivating this organism. Its optimal growth temperature is between 30 and 34°C and pH 6.0- 7.0 (Park et al., 1991).

**Table 2-1: Characteristics of Methanotrophs (Hanson and Hanson, 1996)**

Characteristic	Type I	Type II	Type X
Cell morphology	Short rods,usually occur singly;some cocci or elipsoids	Crescent-shaped rods,pear-shaped cells, sometimes occur in rosettes	Cocci,often found as pairs
Membrane arranged in bundles of vesicular disks	Yes	No	Yes
Paired membranes aligned to periphery of cells	No	Yes	No
Nitrogen fixation	No	Yes	Yes
RuMP pathway present	Yes	No	Yes
Serine pathway present	No	Yes	Sometimes
Proteobacterial subdivision	Gamma	Alpha	Gamma

RuMP = Ribulose monophosphate pathway

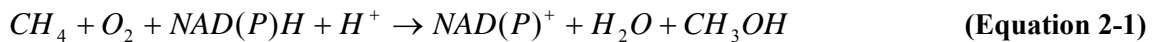
## 2.2 Carbon source for cultivating *M. trichosporium OB3b*

Many studies have been conducted on the growth of *M. trichosporium* and the production of methane monooxygenase however, none have been able to achieve cell densities exceeding 18 g/L (Shah et al., 1996). In that study, *M. trichosporium* was cultivated in batch mode employing nitrogen minimal salts medium containing 10µM copper with

methane as the sole carbon source. Typical growth yields with methane fall within 0.4-0.5 g dry wt. cells/ g methane (Bowman and Sayler, 1994). There have been conflicting reports on the cultivation of *M. trichosporium OB3b* on methanol. Hubley et al., (1975) suggested that the organism could not grow on methanol as a sole carbon source. On the other hand, Best and Higgins (1981) showed that *M. trichosporium* was capable of growing on methanol as a sole carbon source at concentrations of up to 4% v/v. Some studies have shown that *M. trichosporium* grown on methanol retains sMMO activity (Cornish et al., 1984; Fitch et al., 1996; Mehta et al., 1989).

### **2.2.1 Methane metabolism**

Methane is hydroxylated to methanol by methane monooxygenase in a NAD(P)H dependent reaction (Anthony 1982; Cornish et al., 1984; Hanson and Hanson, 1996; Lipscomb 1994; Sullivan et al., 1998).



### **2.2.2 Methanol metabolism**

Methanol, either from the metabolism of methane or externally supplied is oxidized via methanol dehydrogenase (MDH) to formaldehyde (Figure 2-1). The specificity of MDH is restricted to primary alcohols and is activated by ammonia or methylamine (Anthony 1982). The optimal pH for MDH is pH 9, but the enzyme is stable at pH 4.0. MDH is also capable of catalyzing the oxidation of formaldehyde to formate (Anthony 1982;

Sullivan et al., 1998). Formaldehyde is then assimilated into the cell mass via the serine pathway (Figure 2-2).

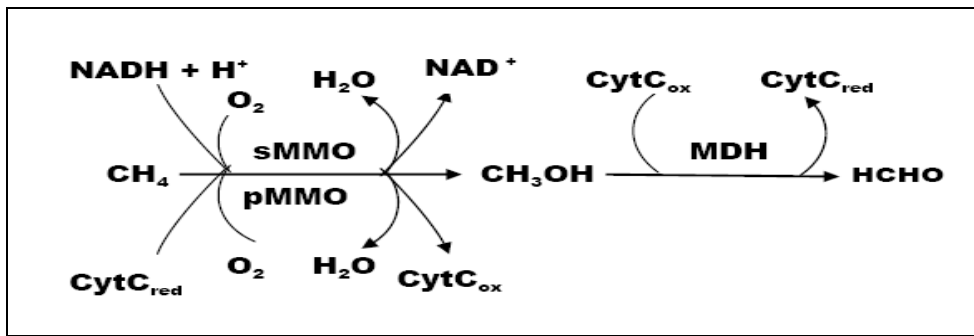


**Figure 2-1:** Oxidation of methane to formaldehyde (Hanson and Hanson, 1996). MDH is methanol dehydrogenase, MMO is methane monooxygenase (s: soluble, p: particulate). CytC is cytochrome (red –reduced, ox –oxidized).

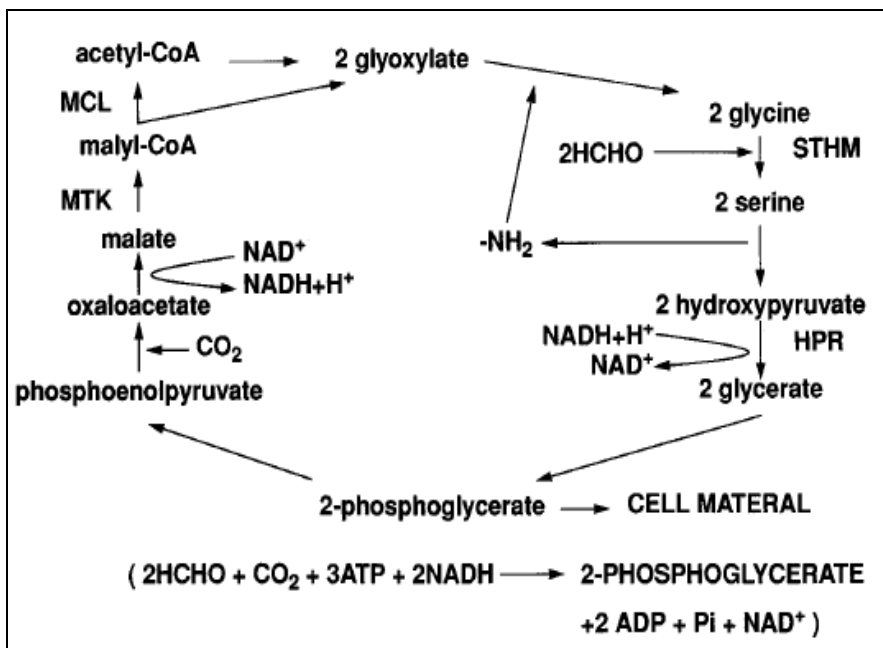


**Figure 2-2:** Serine pathway for the assimilation of formaldehyde in Type II methanotrophs (Hanson and Hanson, 1996). Reactions catalyzed by enzymes unique to Type II methanotrophs are: Serine hydroxymethyl transferase (STHM), hydroxypyruvate reductase (HPR), malate thiokinase (MTK), and malyl coenzyme A lyase (MCL).

### **2.2.3 Formaldehyde assimilation (serine pathway)**

The serine pathway (Figure 2-2) for formaldehyde assimilation is a characteristic which differentiates Type II from Type I methanotrophs. Through a series of steps in the first half of the serine pathway, two molecules of formaldehyde and two molecules of glycine produce two molecules of phosphoglycerate. One molecule of 2-phosphoglycerate is incorporated into cellular material, while the other molecule is converted to phosphoenolpyruvate (PEP). The reaction of fixing carbon dioxide with PEP (catalyzed by phosphoenolpyruvate carboxylase) and reduction of oxaloacetate to malate are similar to reactions in several heterotrophic bacteria (Hanson and Hanson, 1996). The intermediate products of the serine pathway, which consist of carboxylic acids (e.g. glyoxylate, oxaloacetate and malate) and amines (serine and glycine) differ from carbohydrate intermediates formed in other formaldehyde assimilation pathways such as the ribulose monophosphate (RuMP) pathway in Type I methanotrophs (Anthony, 1982).

## **2.3 Effect of other nutrients on growth**

### **2.3.1 Effect of nitrogen source**

#### **2.3.1.1 Ammonium**

King and Schnell (1994) and Whittenbury et al., (1970) have shown that ammonium inhibits methane uptake rates, since ammonia and methane compete for the same active site on MMO. According to Hubley et al., (1975) and King and Schnell (1994), the first product obtained from the oxidation of ammonium, hydroxylamine has a reversible

inhibitory effect on MMO at concentrations as low as 0.1 mM. Furthermore, nitrite which is easily produced from hydroxylamine also negatively affects the growth of cells by inhibiting formate dehydrogenase (Jollie and Lipscomb, 1991), which catalyzes the production of NADH. Whittenbury et al. (1970) reported that with an initial ammonium chloride concentration of 9.4 mM, the concentration of nitrite produced (7 $\mu$ M) was non-inhibitory to cell growth or methane uptake rates of *M. trichosporum* OB3b. This is in agreement with data published by Yoshinari (1985), which proposed that in a batch system, an initial concentration of 10mM ammonia and an accumulation of up to 50  $\mu$ M nitrite, had no significant effect on the growth of *M. trichosporum* cells. However, Shah et al., (1992) showed that concentrations of nitrite higher than 1mM were inhibitory to cell growth. Nitrite has also been tagged as being a product inhibitor of both ammonia and hydroxylamine oxidation in *M. trichosporum* (O'Neill and Wilkinson, 1977). There is no evidence in literature of an adverse effect of ammonium, or nitrite on methanol dehydrogenase.

### 2.3.1.2 Nitrate

Bowman and Sayler (1994) showed that the nitrate concentration range most favorable for cell growth as well as sMMO production is 2 – 100 mM in a copper free medium. The authors claim that no further significant changes in cell growth, yields or sMMO activity was observed with nitrate levels exceeding 100 mM, but no data was shown to corroborate the claim. Park et al., (1992) compared maximum growth rates at two levels of nitrate concentration. The growth rate was found to decrease from 0. 12 h<sup>-1</sup> to 0.08 h<sup>-1</sup>

when *M. trichosporium* was cultivated in medium containing 10 and 40 mM nitrate respectively.

### 2.3.1.3 Nitrogen fixation

It has been proven that nitrogenase can be induced under ammonia and/or nitrate limiting conditions, making *M. trichosporium OB3b* capable of fixing gaseous nitrogen (Chen and Yoch, 1987; Chen 1988). Once nitrate was depleted during the batch cultivation of *M. trichosporium OB3b*, a switch to nitrogen fixation occurred resulting in diauxic growth (Park et al., 1991). The effect of ammonium on nitrogen fixation of four different methanotrophs (including *M. trichosporium OB3b*) was investigated by Murrel (1988). A rapid repression of nitrogenase was observed when ammonium chloride was introduced into the growth medium. Since nitrogen fixation is a less energetically-favorable pathway for nitrogen assimilation, the nitrogenase system is repressed when other inorganic forms of nitrogen are present (Murrel and Dalton, 1983). However, Shah et al., (1992) observed an active nitrogenase system in the presence of nitrate up to 50 mM, implying that cells of *M. trichosporium OB3b* were able to derive cellular nitrogen from both nitrate and gaseous nitrogen.

In comparing the use of ammonium or nitrate as nitrogen sources, a slightly higher theoretical cell yield on carbon is expected when ammonium instead of nitrate is used (Leak and Dalton, 1986). Experimental data published by Chu and Alvarez-Cohen (1998) showed very similar growth rates ( $0.026\text{ h}^{-1}$  and  $0.025\text{ h}^{-1}$ ) for ammonium and

nitrate-grown cells of *M. trichosporium OB3b* respectively, but a lower growth rate (0.02 h<sup>-1</sup>) in nitrogen fixing cultures.

### **2.3.2 Effect of phosphate**

High levels of phosphate inhibit methanol dehydrogenase (MDH) which catalyzes the oxidation of methanol to formaldehyde in methanotrophs (Mehta et al., 1987). Phosphate concentrations between 2 – 25 mM were found to be optimal for cell growth and sMMO activity (Bowman and Sayler, 1994). Park et al., (1991) claimed phosphate concentrations exceeding 40 mM are inhibitory to cell growth. An inhibition of MDH would result not only in starvation, but could also lead to cell death due to accumulation of methanol, hence the importance of maintaining an optimal phosphate concentration (Kim et al., 2003; Mehta et al., 1989).

### **2.3.3 Effect of supplemental CO<sub>2</sub> on lag phase**

Addition of carbon dioxide (as a gas or as bicarbonate) to a bioreactor has been found to decrease the initial lag period (Park et al., 1991). Based on the serine pathway by which *M. trichosporium OB3b* utilizes formaldehyde for cell growth, one molecule of CO<sub>2</sub> is required for every two molecules of formaldehyde assimilated to convert phosphoenol pyruvate to oxaloacetate. An external supplement of CO<sub>2</sub> is necessary for the support of rapid cell growth especially when the medium is sparged with air since this strips off some of the initial CO<sub>2</sub> produced during metabolism. However as cell density increases,

the CO<sub>2</sub> concentration increases and ultimately becomes adequate for rapid growth (Park et al., 1991).

#### **2.3.4 Effect of metal ions and trace nutrients on growth**

Different types of nutrient media with varying compositions of metal ions and trace elements have been utilized for the cultivation of *M. trichosporium OB3b*, yet there are few studies that detail the effects and/or yields of these components on growth of *M. trichosporium OB3b*. Park et al., (1991) concluded that cells require a minimum of 40 µM iron (Fe<sup>2+</sup>) for significant cell growth and that the yield of biomass from iron was 1300 g dry wt cells/ g Fe<sup>2+</sup>. In another study, Shah et al., (1992) demonstrated that in the presence of copper, cells exhibit a higher overall growth rate. When 1 and 10 µM copper were introduced into the bioreactor, the steady state cell density increased by 25% and by 30% respectively. At higher concentrations, copper was inhibitory and the cell growth rate declined. Copper is also known to inhibit the production of sMMO (Davis et al., 1987; Park et al., 1992; Stanley et al., 1983). At low biomass densities, 1 µM of copper is sufficient to completely inhibit sMMO (Park et. al. 1992). Bowman and Sayler (1994) claim that carbon, nitrogen, phosphate, iron and magnesium contribute the most significantly to the growth of *M. trichosporium OB3b* and the expression of sMMO. Other trace elements in the NMS media (Cornish et al., 1984) had no significant effect on growth rates and sMMO expression. However Bowman and Sayler (1994) did not determine the yields of biomass from the trace elements.

## **2.4 Soluble methane monooxygenase**

Soluble methane monooxygenase is a NADH dependent enzyme that is produced in the cell cytoplasm. The expression of this enzyme is the primary reason *M. trichosporium OB3b* is important in the field of bioremediation. The low substrate specificity of sMMO makes it useful in co-metabolic degradation of a host of contaminants such as TCE (Brusseau et al., 1990; Tsien et al., 1989), naphthalene (Cardinal and Stenstrom, 1991) and dichloroethane (Oldenhuis et al., 1989). The exact mechanism of enzyme induction or production is unknown. At low concentrations of copper, sMMO is readily produced, however when transferred to a medium with high copper to biomass ratio, the production of sMMO is suppressed and a switch to pMMO synthesis occurs (Stanley et al., 1983; Stephen et al., 1985).

The precise ratio of biomass to copper at which complete inhibition of sMMO occurs is uncertain, however based on data by Morton et al., (2000), the copper to biomass ratio that resulted in complete sMMO inhibition is approximately 8.5  $\mu$ moles copper/g protein. Assuming cell protein makes up 70% of cell mass (Bowman et. al 1994), the minimum copper to biomass ratio required for complete enzyme inhibition is estimated to be approximately 6  $\mu$ moles copper/g cell dry weight.

### **2.4.1 Enzyme structure**

The MMO enzyme consists of three components, component A which is a hydroxylase (MMOH, 245 kDa) containing non-haem iron, component B (15.8kDa) and component C

which is a reductase (38.4 kDa) containing FAD and an Fe<sub>2</sub>S<sub>2</sub> cluster (Fox et al., 1989). The active site of oxygenase activity is located in the hydroxylase component and the MMOH component of the enzyme catalyzes methane oxidation. The reductase component contributes to electron transport, catalyzing reduction of some acceptors in the hydroxylase and is rapidly reduced by NADH and may be the site of NADH interaction. The third part of the enzyme, component B is a colorless protein which is essential for enzyme activity. Although component B is not required in the oxygenase reaction, the specific activity of the sMMO enzyme is increased by 150 fold when component B is present (Fox et al., 1989). A diagram of the hydroxylase component of the enzyme is provided in (Figure 2-3).

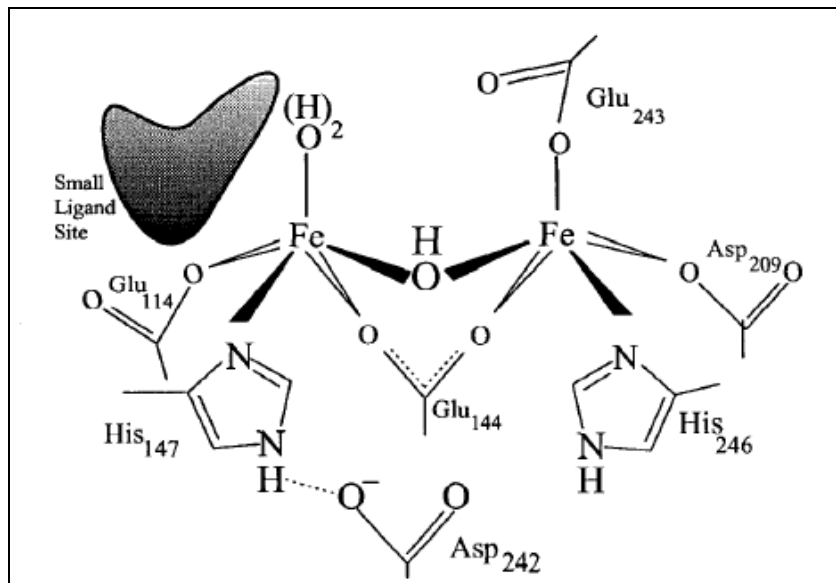


**Figure 2-3: Hypothetical structure of the active-site of MMOH (Lipscomb, 1994).**

#### **2.4.2 Known inhibitors of sMMO**

The inhibitory effect of twelve metal ions on *in vitro* sMMO activity from *M. trichosporium OB3b* was investigated by Jahng and Wood (1996). Copper (I&II), zinc (II) and nickel (II) were found to be major inhibitors of whole cell sMMO activity. Copper (I&II) had the most severe effect on the enzyme, inhibiting both the reductase and hydroxylase components. Zinc (II) was shown to have a negative effect on the hydroxylase component of the sMMO enzyme, whilst nickel (II) decreased the activity of both the hydroxylase and reductase components. Alkaline metals, calcium (II) and magnesium (II) did not exhibit any inhibitory effects at the concentrations investigated. An earlier study by (Stanley et al., 1983) on *Methylococcus capsulatus (Bath)*, investigated the effect of inhibitors at 0.1 mM on both pMMO and sMMO. Ethyne (3% v/v) completely inhibited both enzymes, whilst thiourea inhibited only pMMO.

A summary of the inhibitory effects of growth nutrients on *M. trichosporium OB3b* is provided in Table 2-2.

**Table 2-2: Effect of medium components on *M. trichosporium OB3b***

Component	Range	Effect	Reference
methanol	> 4 % v/v	growth inhibition	Best and Higgins, 1981
copper	> 10 µM > 0.25 µM	growth inhibition sMMO inhibition	Park et al., 1991 Brusseau et al., 1990
ammonium	all	competes for active site of MMO	Hubley et al., 1975 King and Schnell, 1994
	< 10 mM	optimal for growth	Whittenbury et al., 1970 Yoshinari, 1985
nitrate	2 - 100 mM	optimal for growth	Bowman and Sayler, 1994
phosphate	> 40 mM	growth inhibition	Park et al. 1991
Fe <sup>2+</sup>	40 - 80 µM	optimal for sMMO activity and cell growth	Park et al. 1991

## **Chapter 3**

### **Online methanol measurement**

Methanol, despite being completely soluble in water, is an inhibitory substrate and is toxic to cells at high concentrations. Hence, it is important to control the methanol concentration below inhibitory/toxic levels. Online methods of analyzing methanol tend to be more direct and rapid. Offline techniques such as gas chromatography (GC), high performance liquid chromatography, infrared spectroscopy and mass spectroscopy tend to be labor intensive and may require sample preparation. For instance, in order to obtain an accurate GC measurement of methanol, a liquid sample may need to be centrifuged and the supernatant mixed with a known aliquot of an internal standard before it is analyzed.

A vapor phase sensor is an alternate and inexpensive method of measuring methanol concentration online. These sensors detect and quantify methanol concentration in the vapor phase, which can then be related to liquid phase concentrations. The Figaro TGS822 volatile gas sensor has been widely used in the detection of alcohols. The sensor is typically placed in the reactor air outlet (Katakura 1998). Unfortunately, they are sensitive to humidity. As water adsorbs on the sensor surface, it decreases the detector active area causing drift in the sensor output.

In this study, an *in situ* probe was constructed and equipped with the Figaro TGS822 sensor to minimize the effect of water aerosols on the sensor. This chapter discusses the experimental set-up, the control configuration, the sensor dynamics and performance.

### **3.1 Materials and methods**

#### **3.1.1 Online methanol control**

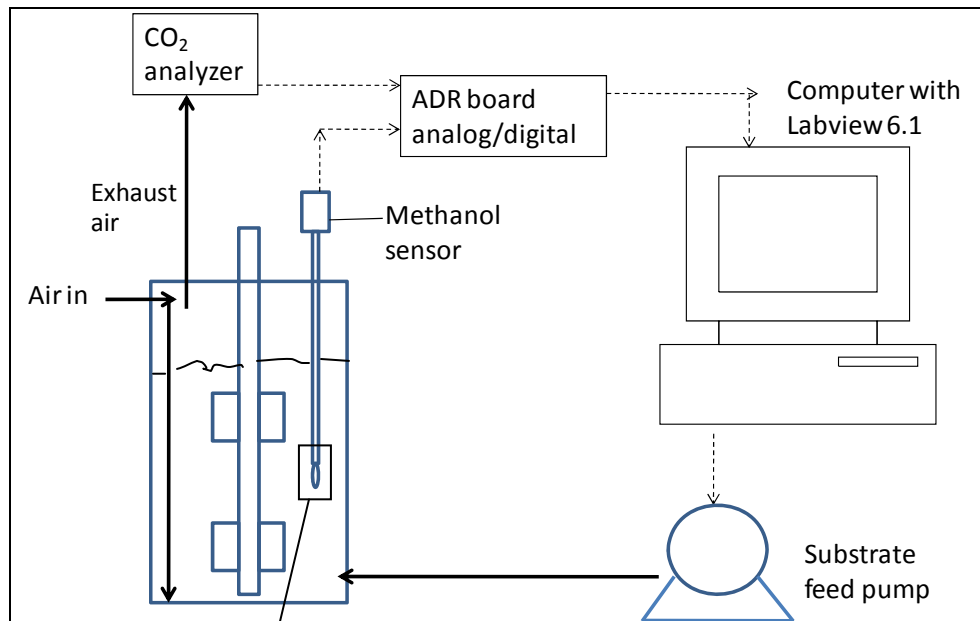
The methanol control system consisted of an autoclavable probe containing a Figaro TGS822 sensor, an analog/digital board (ADR 2000, Ontrak Control Systems, Sudbury, Ontario), computer, Labview 6.1 as the control program, and a peristaltic pump (Figure 3-1 A). The sensor contains a heated SnO<sub>2</sub> surface, in the presence of methanol or any reducing gas, the electrical resistance of SnO<sub>2</sub> decreases and the change in resistance can be measured and related to gas concentration.

#### **3.1.2 Experimental set-up**

##### **3.1.2.1 Growth medium**

A study by Ramon et al., (2004) showed an offset in methanol measurements by the TGS822 sensor when determining methanol concentration in culture medium rather than distilled water. Therefore the liquid medium used for characterizing the probe was the same as that used in cultivating *M. trichosporium OB3b*. Since ammonium hydroxide was utilized for pH control, the culture medium which was based on that of Cornish et al., (1984) was modified to use ammonium sulfate as the nitrogen source; 0.66 g/L (NH<sub>4</sub>)<sub>2</sub>SO<sub>4</sub>, 0.53 g/L KH<sub>2</sub>PO<sub>4</sub>, 1.62 g/L Na<sub>2</sub>HPO<sub>4</sub>.7 H<sub>2</sub>O, 7 mg/L CaCl<sub>2</sub>.2H<sub>2</sub>O, 37 mg/L MgSO<sub>4</sub>.7 H<sub>2</sub>O, 11.2 mg/L FeSO<sub>4</sub>.7H<sub>2</sub>O, 0.574 mg/L ZnSO<sub>4</sub>.7H<sub>2</sub>O, 0.446 mg/L MnSO<sub>4</sub>.7H<sub>2</sub>O, 0.124 mg/L H<sub>3</sub>BO<sub>3</sub>, 0.096 mg/L NaMoO<sub>4</sub>.2H<sub>2</sub>O, 0.096 mg/L CoCl<sub>2</sub>.6H<sub>2</sub>O, and 0.166 mg/L KI.

A.



B.

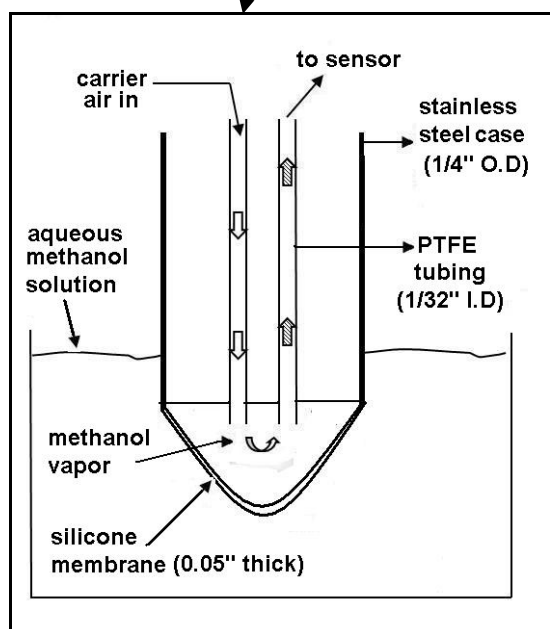


**Figure 3-1: (A) Methanol control system.  
(B) Schematic of methanol probe**

### **3.1.2.2 Bioreactor**

A 5 L stirred tank Minifors bioreactor (Infors-HT, Bottmingen, Switzerland) was utilized for all experiments. The pH was controlled at  $6.8 \pm 0.02$  and agitation speed at 500 rpm.

### **3.1.2.3 Operating temperature**

Temperature fluctuations affect the rate of chemical reaction on the sensor detector surface, hereby changing the sensor output (Figaro Engineering Inc. 2004) and since methanol evaporation is also affected by temperature changes, the temperature of the bioreactor was maintained at  $30 \pm 1$  °C, which is the optimal temperature for cultivating *M. trichosporium OB3b* (Lee, et al 1996; Park et al., 1991).

### **3.1.3 Online methanol detection**

The probe design was based on the methanol sensor of Wagner et al., (1997) and the ethanol sensor of Noronha et al., (1999). The probe consists of a hollow cylindrical stainless steel tube (1.5 ft long and 1/4" O.D), with a silicone membrane attached to one end. Inside the tube are two identical PTFE 1/32" tubings, which are in close proximity to the silicone membrane and extend to the other end of the steel casing into a compartment which houses the Figaro sensor (Figure 3-1 B). One length of PTFE tubing transports air into the membrane chamber while another conveys the air/methanol mixture from the membrane chamber to the sensor. The membrane is 0.05" thick silicone which is permeable only to gases. During operation, the membrane end of the probe is immersed in the liquid medium and methanol diffuses through the membrane to the sensor. Upon

detection, an analog signal (in Volts) is sent from the sensor to the ADR board which converts it to a digital signal that can be read by the computer. Calibrations were performed by adding known amounts of 100% methanol into known volumes of nutrient medium in a bioreactor and correlating the liquid methanol concentrations to the sensor output in volts.

### **3.1.4 Offline methanol verification**

The Figaro sensor measurements were verified by analyzing the methanol concentration in liquid samples offline with a Hewlett-Packard gas chromatograph (GC), 0.1 mL of 1% butanol was added to each sample as an internal standard. The gas chromatograph was equipped with a Cabowax®-PEG column and a flame ionization detector. The methanol concentration was determined by relating ratios of peak areas to those of known standards. The column temperature was initially held at 60 °C for 1 min and then increased to 150 °C at 30 °C /min. The injector and detector temperatures were kept constant at 150 °C and 250 °C respectively.

### **3.1.5 Sensor characterization**

Following step changes in methanol concentration, the average response time was determined by measuring the time it took for the sensor output to achieve a new steady state. The air flow rate through the probe was varied at 19, 40 and 60 ( $\pm 1.5$ ) mL/min

with a rotameter to determine its effect on the sensor output. The lowest flow rate was based on the range tested by Guarna et al., (1997).

### **3.1.6 Sensor performance**

Online methanol measurements from the sensor were compared to values obtained from offline GC analysis of samples during fed-batch cultivation of *M. trichosporium OB3*. Samples containing biomass were centrifuged at 10,000 xg for 10 min and the supernatant was then analyzed for methanol with the GC. During the fermentation, measurements from the methanol sensor were used in a simple feedback control to prevent methanol concentration from exceeding 2 g/L. If methanol levels exceed 2 g/L, a signal is sent to the pump to switch off methanol feeding. The initial composition of the liquid medium was the same as outlined in section 3.2.1, however the composition varied during the course of the fed-batch experiment. Biomass density and CO<sub>2</sub> production increased during the experiment. The initial airflow through the reactor was 2 ± 0.08 L/min, and was gradually increased (up to 2.25 L/min) to maintain dissolved oxygen above 40 % saturation.

## **3.2 Results and discussion**

### **3.2.1 Sensor characterization**

The response time is highly dependent on the methanol vaporization rate, mass transfer rates across the silicone membrane and air flow rate through the probe. Since the rate of methanol volatilization is affected by temperature and pressure both were kept constant for every experiment. Given that the air flow rate through the probe affects how fast methanol vapor is delivered from the membrane chamber to the sensor, an increase in airflow was expected to decrease the response time. The effect of air flow (19, 40 and 60 mL/min) through the probe was investigated. A step change in liquid methanol concentration from 1 to 2 g/L resulted in similar sensor response times (approximately 12 min) at each flow rate (Figure 3-2). There was negligible effect of the corresponding residence times at the different flow rates because the actual residence time in the probe was quite low in comparison to the overall response time. At a flow rate of 19 ml/min it takes approximately 0.5 seconds to transport methanol from the membrane chamber to the sensor (calculated based on the probe length of 1.5 ft and PTFE tube diameter of 1/4") and 0.15 seconds at a flow rate of 60 mL/min. This indicates that the limiting factor is mass transfer across the silicone membrane. In Figures 3-2 and 3-3, it can be observed that sensitivity of the sensor output had decreased with increasing air flow rate. A flow rate of 19 mL/min was fixed for subsequent studies.

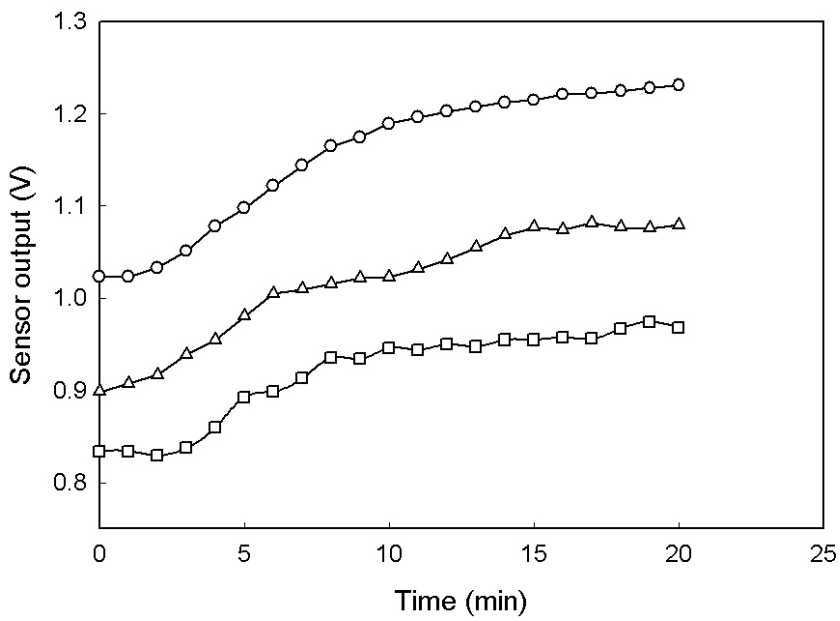


**Figure 3-2:** Response time of sensor to a step change in methanol concentration from 1 to 2 g/L at 0 min. The effect of 19 mL/min ( $\circ$ ), 40 mL/min ( $\Delta$ ) and 60 mL/min ( $\square$ ) carrier air flow rates, is shown.

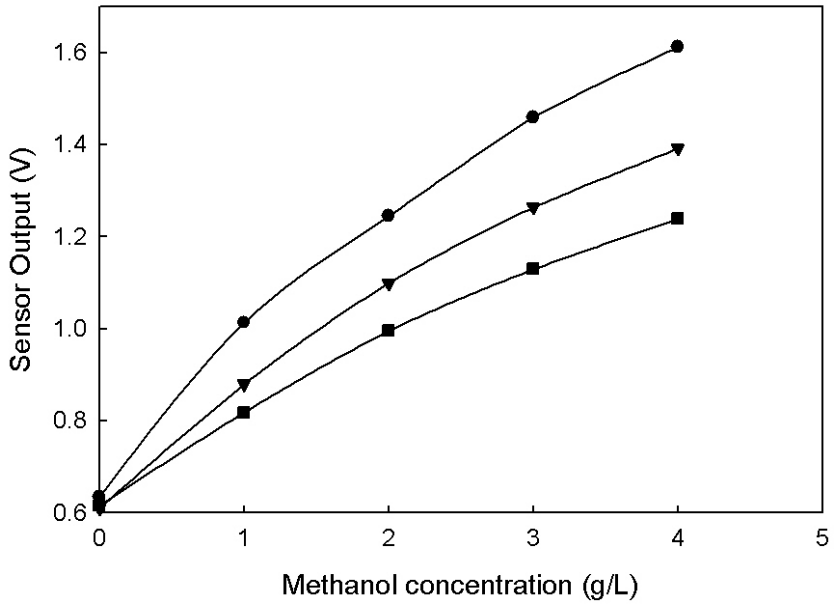


**Figure 3-3:** Sensitivity to airflow rate through probe: 19 mL/min ( $\bullet$ ), 40 mL/min ( $\nabla$ ) and 60 mL/min( $\blacksquare$ )

The response of the sensor to changes in methanol concentrations was not linear (Figure 3-3). The non-linearity response of the sensor was expected as sensor specifications in the manufacturer's catalog indicated a logarithmic relationship between sensor resistance and gas concentration within the detection limits. The explanation for the non-linear response of the sensor has been provided in detail elsewhere (Figaro Engineering Inc. 2004; Guarna et al., 1997; Heiland 1982; Jones et al., 1985; Morrison 1982; Watson 1984). The non-linear response is due to a combination of effects. The first is a result of the electronic measuring circuit (Appendix A) that makes use of a voltage divider configuration to quantify changes in conductance of the detecting element ( $\text{SnO}_2$ ) which yields a parabolic relationship between output voltage and conductance. The second effect is a result of the non-linear physical-chemical interaction between the detector, oxygen and methanol. The conductivity of a sintered semiconductor such as  $\text{SnO}_2$  is primarily affected by the electrons populating the surface states. Hence changes in the availability of the surface states alter the conductivity. For the methanol sensor, in the absence of methanol, the chemisorption of oxygen depletes the conduction electrons available at the surface which lowers the overall conductivity. When methanol is in contact with the detector, it adsorbs to the surface and the semiconductor catalyzes the reduction of surface-bound oxygen, producing the more weakly interacting formaldehyde that desorbs and frees surface conduction band electrons which in turn, increases the measured conductivity (Guarna et al., 1997).

### **3.2.2 Sensor performance**

Figure 3-4 shows methanol concentrations determined by the sensor and the offline GC analysis over the duration of a fed-batch fermentation. The sensor provided satisfactory measurement of the methanol concentration during the course of the fed-batch fermentation until about 80 h of operation, the sensor output deviated from the offline GC analysis. This drift in performance was also observed by (Ramon et al., 2004) during the high cell density cultivation of *Pichia pastoris*. In the current study of the high cell density cultivation of *M. trichosporium OB3b*, the airflow through the bioreactor was increased automatically to maintain the dissolved oxygen level above 40% saturation. This increase in airflow caused a slight rise in methanol vaporization which resulted in an offset in the sensor calibration probably causing the deviation in Figure 3-4. The sensor, although not as accurate as the GC analysis, can provide an adequate method of controlling methanol concentration if it is regularly recalibrated online. A one point calibration can be performed by using another method (such as GC) to measure the methanol concentration.

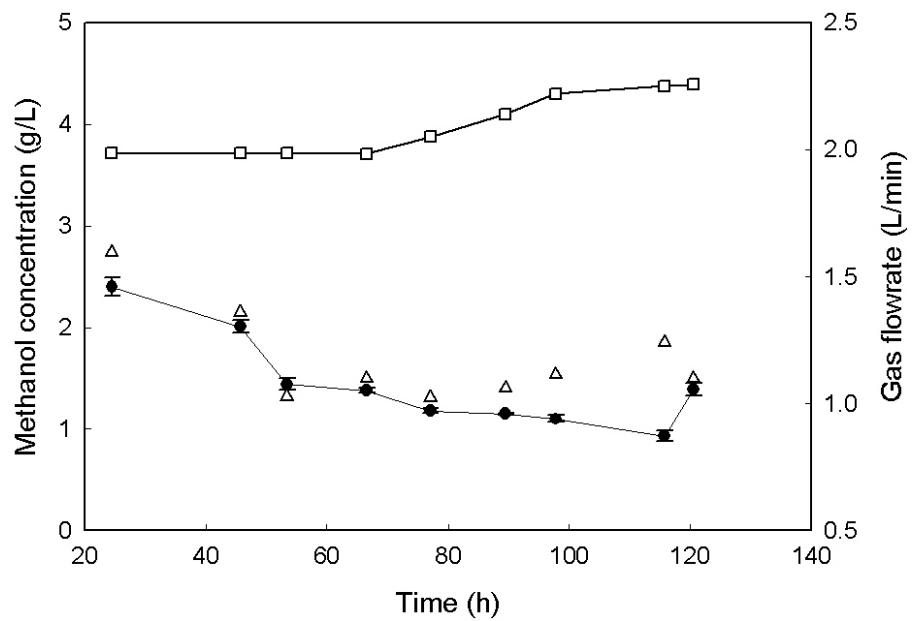


**Figure 3-4: Sensor performance during fermentation. Methanol measured with sensor ( $\Delta$ ), with gas chromatography ( $\circ$ ) and total airflow rate through the bioreactor ( $\square$ ).**

### **3.3 Conclusions**

During a methanol fed-batch cultivation of *M. trichosporium OB3b*, in the first 80 h, the sensor provided an adequate means of estimating the bulk liquid methanol concentration. However, the sensor cannot be used as a stand-alone method for accurate liquid methanol analysis during fed-batch fermentation, because of the constantly changing environment. It is probable that salt concentrations (which vary over the course of the fermentation), and air flow rate through the reactor may affect the dynamics of the methanol liquid-vapor system. Consequently, further studies should be carried out on the effects of these factors on sensor response.

The long response time of 12 min is a source of concern because at higher biomass densities, the rate of methanol uptake by cells increases and this could potentially introduce a larger error in the estimation of methanol concentration in the bioreactor. This problem can be reduced by the use of a more permeable material or a thinner membrane.

## **Chapter 4**

### **High cell density cultivation of *Methylosinus trichosporium OB3b* on methanol**

This chapter covers high cell density cultivation of *M. trichosporium OB3b* on methanol.

The effects of medium components on growth were investigated and biomass yields were determined and used to adjust the composition of the feed medium for fed-batch operation.

#### **4.1 Materials and methods**

##### **4.1.1 Culture maintenance**

*M. trichosporium OB3b* was maintained on Noble agar plates containing Higgin's nitrogen minimal salts (Cornish et al., 1984) or Femi's medium A, B or C (Table 4-1).

The plates were incubated at  $30 \pm 1$  °C in an air tight vessel containing a methane-air (4:1) atmosphere which was replenished twice a week. Plates were also prepared with 0.1 g/L cycloheximide to prevent fungal contamination and/or 15 µM allylthiourea to stimulate sMMO production.

Purity was verified by checking cultures microscopically and streaking cultures on nutrient agar plates.

**Table 4-1: Composition of the four culture media used in this study**

Nutrient	Concentration (mg/L)			
	Higgin's medium	Medium A	Medium B	Medium C
NaNO <sub>3</sub>	850	-	-	850
(NH <sub>4</sub> ) <sub>2</sub> SO <sub>4</sub>	-	660	490	-
KH <sub>2</sub> PO <sub>4</sub>	530	530	125	125
Na <sub>2</sub> HPO <sub>4</sub> .7H <sub>2</sub> O	1620	1620	351	351
CaCl <sub>2</sub> .2 H <sub>2</sub> O	7.0	7.0	6.25	6.25
MgSO <sub>4</sub> .7 H <sub>2</sub> O	37	37	44	44
Fe SO <sub>4</sub> .7 H <sub>2</sub> O	11.0	11.0	10.2	10.2
Zn SO <sub>4</sub> .7 H <sub>2</sub> O	0.57	0.57	0.47	0.47
Mn SO <sub>4</sub> .7H <sub>2</sub> O	0.45	0.45	0.37	0.37
H <sub>3</sub> BO <sub>3</sub>	0.12	0.12	0.12	0.12
NaMoO <sub>4</sub> .2H <sub>2</sub> O	0.10	0.10	1.18	1.18
COCl <sub>2</sub> .6H <sub>2</sub> O	0.10	0.10	0.06	0.06
KI	0.17	0.17	0.17	0.17

Higgins medium (Cornish et al., 1984) excluding K<sub>2</sub>SO<sub>4</sub>.

Medium A is similar to Higgin's medium, but NaNO<sub>3</sub> is replaced with (NH<sub>4</sub>)<sub>2</sub>SO<sub>4</sub> as the nitrogen source. The concentration of trace nutrients in Medium B and Medium C were modified according to biomass yield ratios.

#### 4.1.2 Analytical methods

##### 4.1.2.1 Biomass

Biomass densities (g/L) were determined by measuring absorbance at 600 nm in a spectrophotometer (Spectronic Unicam UV1, Fisher Scientific Nepean, ON). A linear (0-0.12 g/L dry wt) calibration curve (Appendix B, Figure B-1) was obtained by relating the mass of known aliquots of lyophilized cells to a corresponding optical density at 600 nm. An optical density of 1 at A<sub>600</sub> was equivalent to 0.389 mg dry cell wt /mL.

#### 4.1.2.2 Methanol

Online analysis was performed using the Figaro TGS 822 vapor phase sensor. A calibration was prepared prior to each fed-batch experiment with known aliquots of methanol. During operation, sensor measurements were verified with offline GC analysis and the sensor was recalibrated (one-point calibration) when necessary.

Methanol in the supernatant of centrifuged (10.000 xg) samples was analyzed offline with a Hewlett-Packard gas chromatograph (GC), 0.1 mL of 1% butanol was added to each sample as an internal standard. The gas chromatograph was equipped with a Cabowax®-PEG column and a flame ionization detector. The methanol concentration was determined by relating ratios of peak areas to those of known standards. The column temperature was initially held at 60 °C for 1 min and then increased to 150 °C at 30 °C /min. The injector and detector temperatures were kept constant at 150 °C and 250 °C respectively.

#### 4.1.2.3 Carbon dioxide

Carbon dioxide from the bioreactor was measured in the air outlet with a Guardian Plus D500 infrared analyzer, Edinburgh Sensors, UK. Data was acquired with an analog signal converter (ADR 2000, Ontrak Control Systems, Sudbury, Ontario) interfaced with a computer using LABVIEW 6.1 (National Instruments) software.

#### 4.1.2.4 Determination of sMMO activity

The sMMO activity was analyzed by the naphthalene oxidation method (Brusseau et al., 1990; Tsien et al., 1989). Biomass samples were centrifuged (10,000 xg for 10 min) and

resuspended in medium C to a cell density of 0.5g/L. Potassium formate (20 mM) was added to serve as an energy source. The samples were then incubated with excess naphthalene crystals at  $30 \pm 1$  °C and 200 rpm for 1 h. The incubated solution was then centrifuged (10,000 xg for 10 min) and the supernatant was tested for naphthol by reaction with 0.1 mL of tetrazotized o-dianisidine to form a purple diazo dye. The mixture was stabilized with 0.4 mL acetic acid. The absorbance was measured within 15 min at a wavelength of 530 nm and correlated to naphthol concentration via a calibration curve freshly prepared with 0 to 7 mg/L 1-naphthol.

#### 4.1.2.5 Phosphate

Biomass samples were centrifuged at 10000 xg for 10 min. The supernatant phosphate concentration was measured via reduction of phosphomolybdate to molybdene blue (Lanzetta et al., 1979). Sodium sulfites and carbonates were added to the mixture to keep proteins dissolved in the liquid phase. The intensity of the blue complex formed is proportional to phosphate concentration and was measured photometrically at 750 nm. For every analysis a new calibration was performed using standards with phosphate concentration ranging from 0 – 0.5 g/L.

#### 4.1.2.6 Nitrate

Following centrifugation of biomass samples (10,000 xg for 10 min), the nitrate concentration in the supernatant was quantified by measuring the absorbance at a wavelength of 220 nm in a UV spectrophotometer (Spectronic Unicam UV1, Fisher Scientific Nepean, ON). Optical density measurements from samples were related to a

standard calibration curve to determine nitrate concentration within a range of 0 – 20 mg/L (Appendix B, Figure B-2).

#### 4.1.2.7 Ammonium

Biomass samples were centrifuged at 10000 xg for 10 min and ammonium ion concentration in the supernatant was determined by the colorimetric phenol-hypochlorite reaction developed by Weatherburn (1967). Reagent 1(2.5 mL) containing 5 g of phenol with 25 g of sodium nitroprusside per 500 mL of water was added to 40 µL of sample, followed by the addition of 2.5 mL reagent 2 (2.5 g sodium hydroxide and 4.2 mL sodium hypochlorite per 500 ml solution). The reactant mixture was incubated at room temperature for 30 min and cooled in a cold water bath (~ 5 -10°C) for 5 min to stop the reaction. After cooling, the absorbance of samples was measured within 30 min at a wavelength of 630 nm. For every analysis a new calibration was performed using standards with ammonium concentration ranging from 0 – 0.4 g/L.

#### 4.1.2.8 Other cations

Supernatant samples were filtered (0.45 µm) and cation ( $\text{Fe}^{2+}$ , $\text{Ca}^{2+}$ , $\text{K}^+$ , $\text{Mn}^{2+}$ , $\text{Mg}^{2+}$  $\text{Na}^+$  and  $\text{Zn}^{2+}$ ) concentrations were determined via inductive coupled plasma analysis with a Varian Vista AX CCD Simultaneous ICP-AES by the Analytical Service Unit, Queen's University.

#### **4.1.3 Shake flask studies: medium optimization**

Cultures cultivated in shake flasks were incubated at 30°C and 200 rpm in an incubator shaker (Innova 44, New Brunswick Scientific, Edison, NJ USA).

##### **4.1.3.1 Effect of methanol concentration on growth**

Studies were carried out in shake flasks to determine the inhibitory effect of methanol concentration on growth of *M. trichosporium OB3b*. NMS medium C (100 mL in 250 mL Erlenmeyer flasks) was utilized for this study. The inoculum (actively growing cells) was prepared in the same medium with methanol as the sole carbon source. Each shake flask was prepared with 10% v/v inoculum and the initial methanol concentration in each growth flask was varied between 0.3 to 80 g/L. Biomass growth was monitored in each flask over the first few days, and the initial specific growth rates at each methanol concentration were compared.

##### **4.1.3.2 Evaluation of initial specific growth rates**

Biomass growth was monitored over the first few days and the initial specific growth rates were obtained from the slope of the normalized natural logarithm of biomass concentration plotted against time according to Equation 4-1.

$$\ln \left( \frac{X_t}{X_0} \right) = \mu \times t \quad (\text{Equation 4-1})$$

Where  $X_t$  is biomass (g/L) at time,  $t$  (h),  $X_0$  is initial biomass (g/L) and  $\mu$  is the specific growth rate ( $\text{h}^{-1}$ )

#### 4.1.3.3 Effect of ammonium on methanol-grown cells

Shake flask experiments were performed to determine the inhibitory effect of ammonium concentration on methanol-grown cells of *M. trichosporium OB3b*. NMS medium B (100 mL in 250 mL Erlenmeyer flasks) was utilized for this study. The inoculum (actively growing cells) was prepared in the same medium with methanol (4 g/L) as the sole carbon source. The initial ammonium concentration was varied between 0.045 and 0.35 g/L. The cells were incubated at 30°C in an incubator shaker (Innova 44, New Brunswick Scientific, Edison, NJ USA). Biomass was measured in each flask over the first few days, and the initial specific growth rates were compared.

#### 4.1.3.4 Effect of antifoam on growth

The effect of different antifoams on growth was investigated in shake flask studies. The first study was performed with Sigma 204, a polypropelyene based antifoaming agent (Sigma Aldrich). Three concentrations (0, 0.01 and 0.1 % v/v) of Sigma 204 in shake flasks containing medium B and 4 g/L methanol were tested. The inoculum was prepared in the same medium without antifoam. However due to the formation of emulsions in growth medium containing Sigma 204, optical density measurements were not reliable growth estimation. Instead, methanol and ammonium uptake were used as an indication of bacterial growth.

In the second study, the antifoaming agents investigated were canola vegetable oil, Sigma O-30 (fatty-acid based) and Sigma SE-15 (silicone based). This experiment

was performed with medium B and the antifoam concentrations investigated were 0, 0.05, 0.1 and 0.2 % v/v.

#### **4.1.4 Bioreactor studies**

Bioreactor experiments were performed in a 5 L Minifors stirred tank reactor (Infors-HT, Bottmingen, Switzerland). The temperature was controlled at 30°C, while the initial agitation was 400 rpm. The pH was controlled at 6.8 and at 6.4 during supplemental CO<sub>2</sub> feeding. Ammonium hydroxide was utilized for automatic pH control as well as a source of additional nitrogen. The dissolved oxygen (DO) was maintained above 40% saturation by adjusting the agitation speed manually and air flow rate automatically (feedback control). The control of DO (via air flow rate), pH, methanol and nutrient feeding was carried out with a data acquisition board (ADR2000 Ontrak Control Systems Inc. Sudbury, ON, Canada) and Labview 6.1 program (National Instruments, Vaudreuil-Dorion, QC, Canada). During lag, supplemental carbon dioxide was included in the air inlet to the reactor to shorten the lag phase.

Two fed-batch cultivation experiments were carried out. A summary of the inoculum preparation and differences in bioreactor operating conditions is provided in Table 4-2. In fermentation 1, the concentration of nutrients was determined over the course of the fermentation and the biomass yields on nutrients (medium A) were determined. These yield values were used to formulate medium B which was utilized in

subsequent fed-batch experiments. The concentration of trace nutrients (concentration < 100 ppm) in medium B was calculated for growth of 4 g/L dry wt. biomass.

**Table 4-2: Summary of operating conditions of two fed-batch fermentation experiments**

Trial	Inoculum	Bioreactor					
		Medium	Operating volume	CO2 supplement	Methanol feeding	Trace Nutrient feeding	Phosphate feeding
Fermentation 1	Higgin's medium	medium A	3.5 L	5 ± 0.05 % (v/v)	Automatic, CCP based	Manual	Manual
Fermentation 2	medium B	medium B	3.5 L	3.5 ± 0.05% (v/v)	Automatic, CCP based	Automatic, Yield based	Manual

CCP: cumulative carbon dioxide production

Trace nutrients include: MgSO<sub>4</sub>.7H<sub>2</sub>O, FeSO<sub>4</sub>.7H<sub>2</sub>O, CaCl<sub>2</sub>.2H<sub>2</sub>O, ZnSO<sub>4</sub>.7H<sub>2</sub>O, MnSO<sub>4</sub>.7H<sub>2</sub>O, H<sub>3</sub>BO<sub>3</sub>, NaMoO<sub>4</sub>.2H<sub>2</sub>O, CoCl<sub>2</sub>.6H<sub>2</sub>O; and KI.

#### 4.1.5 Methanol feeding strategy for fed-batch bioreactor cultivation

Fermentation experiments commenced with an initial methanol concentration of  $2 \pm 0.5$  g/L. Methanol was fed semi-continuously based on cumulative methanol consumption estimation. The cumulative methanol consumption (CMC) was estimated online every 10 seconds (Equation 4-2) based on both real time CCP measurements and yield computation ( $Y_{CO_2/CH_3OH}$ ). The yield of carbon dioxide from methanol was calculated online every 15 min (Equation 4-3). The amount of methanol fed was kept equal to the estimated CMC (Figure 4-1), thus maintaining a constant methanol concentration in the bioreactor. To prevent an accidental overshoot in methanol concentration in the bioreactor, in addition to the CCP feeding strategy, a fail-safe feedback control was implemented. The Figaro sensor was used to detect methanol online and the upper set point limit was 2 g/L methanol. In the event that the methanol concentration exceeds 2 g/L, the methanol feed pump is turned off (Figure 4-2).

$$CMC = \frac{CCP}{Y_{CO_2/CH_3OH}} \quad (\text{Equation 4-2})$$

Where CMC is cumulative methanol consumed (g) at time, t and CCP is cumulative CO<sub>2</sub> produced (g) measured at any time, t.  $Y_{CO_2/CH_3OH}$  is the yield of CO<sub>2</sub> to methanol (g/g).

$$Y_{CO_2/CH_3OH} = \frac{CCP \text{ (g)}}{\text{Total methanol fed (g)} - \text{residual methanol in bioreactor (g)}} \quad (\text{Equation 4-3})$$

Residual methanol in the bioreactor was determined online with the Figaro sensor.

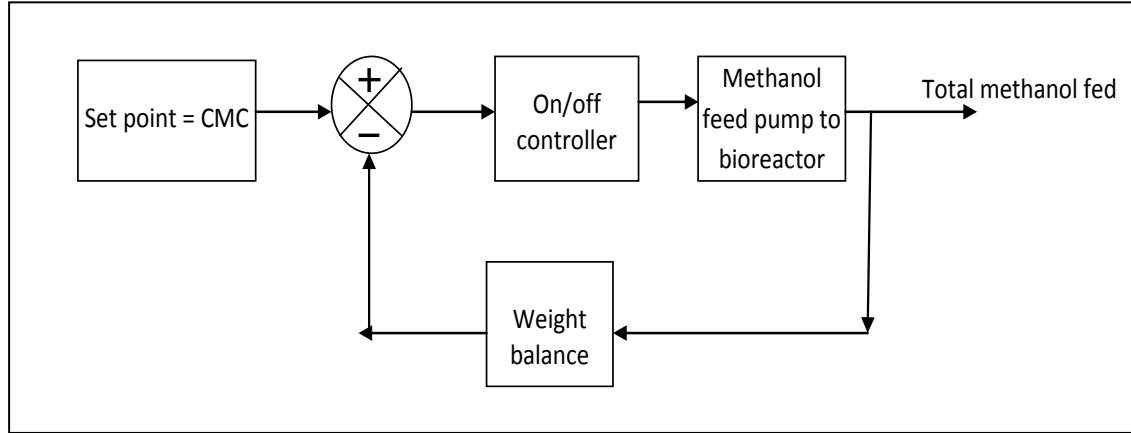


**Figure 4-1: Methanol feeding strategy; CMC = cumulative methanol consumed which was estimated online. The methanol feed pump is on when the total methanol fed is less than the CMC.**

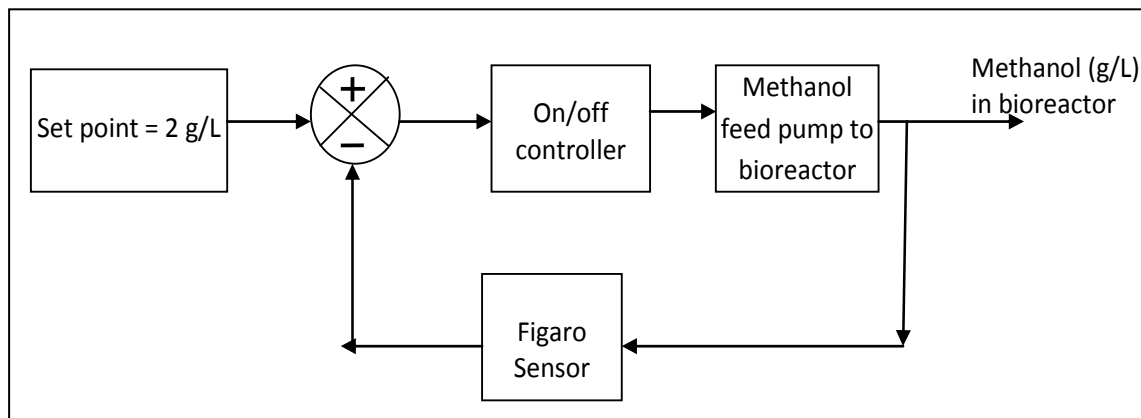


**Figure 4-2: Fail safe methanol control. If methanol in the reactor exceeds 2 g/L, the methanol feed pump is shut off.**

## **4.2 Results and discussion**

### **4.2.1 Shake flask studies: medium optimization**

To achieve high cell density cultivation in a fed-batch reactor, it was necessary to investigate the inhibitory effect of major nutrient components on growth.

#### **4.2.1.1 Effect of methanol concentration on growth**

Studies were carried out in shake flasks with medium C to determine the inhibitory effect of methanol concentration on the growth of *M. trichosporium OB3b* using the initial specific growth rates at each methanol concentration. Cell growth was completely inhibited at methanol concentrations exceeding 40 g/L (Figure 4-3). On the other hand, higher growth rates were achieved at concentrations less than 2 g/L. Hence for high growth rates, methanol should be fed such that the methanol concentration does not exceed 2 g/L.

#### **4.2.1.2 Effect of ammonium on methanol-grown cells**

The initial growth rates decreased from  $0.025\text{h}^{-1}$  to  $0.017\text{ h}^{-1}$  as the initial ammonium concentration increased from 0.045 g/L to 0.33 g/L respectively (Figure 4-4). The data suggests the inhibitory effect of ammonium can be reduced by using low concentrations. To reduce inhibition and avoid ammonium limitation, the ammonium concentration in fed-batch studies should be controlled between 0.035 -0.10 g/L.

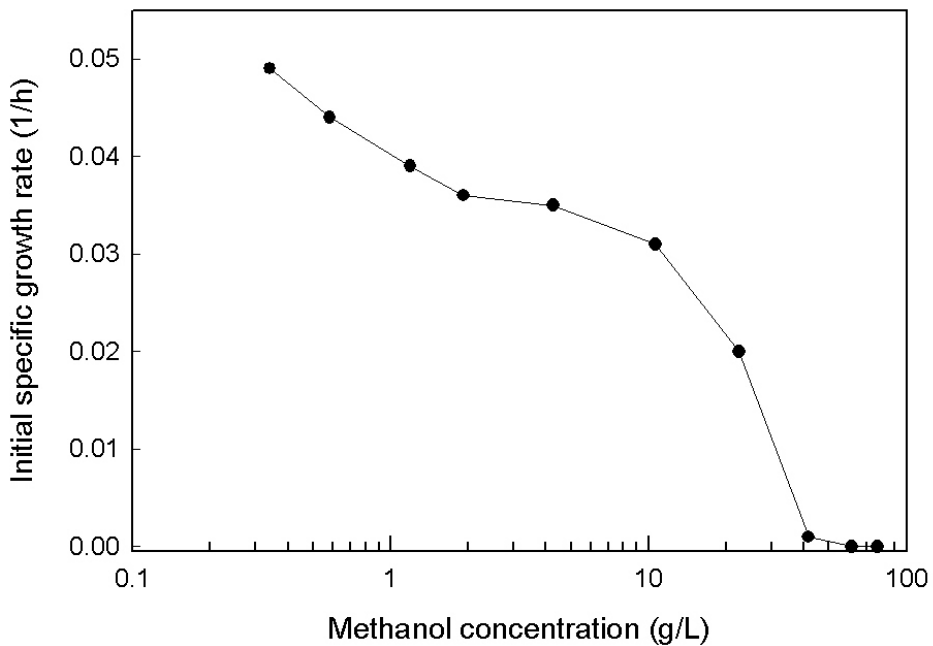


**Figure 4-3: Inhibitory effect of methanol on growth of *M. trichosporium OB3b*:** Shake flasks containing 100 mL medium C and varying levels of methanol were prepared with equal volumes of actively growing biomass from the same inoculum.

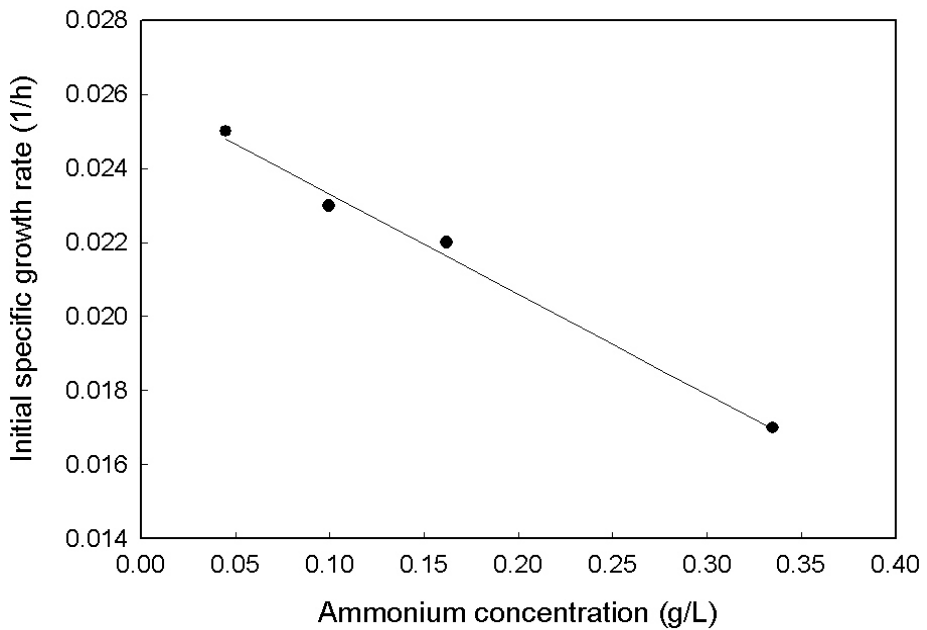


**Figure 4-4: Inhibitory effect of increasing ammonium levels on growth rate of *M. trichosporium OB3b***

#### 4.2.1.3 Effect of antifoam

Sigma 204 was the initial choice of antifoam 204. The effect of Sigma 204 concentrations (0, 0.01 and 0.1% v/v) on cell growth after 5 days was investigated in shake flasks containing medium C with an initial methanol concentration of 4 g/L. From Table 4-3, it can be observed that a concentration of Sigma 204 as low as 0.01% (v/v) had a negative impact on both carbon and nitrogen uptake. It appears to have a considerably higher effect on ammonium uptake. It is probable that the inhibitory effect of increasing Sigma 204 concentration is due to the formation of hydrophobic boundaries as a result of binding of the polypropylene based antifoam to lipid cell membranes which prevented cell access to polar species such as ammonium.

**Table 4-3: Effect of antifoam Sigma 204 on methanol and ammonium uptake**

Antifoam concentration (% v/v)	Methanol (%) Utilized	NH <sub>4</sub> (%) Utilized
0.00	86 ± 1.8	74 ± 3.0
0.01	34 ± 20	3.1 ± 1.9
0.10	25 ± 7.7	0.74 ± 0.38

Once Sigma 204 was found to be inhibitory to *M. trichosporium OB3b*, other antifoams (vegetable oil, Sigma O-30 and Sigma SE-15) were investigated. Vegetable oil appeared to affect the uptake of both ammonium and methanol in a similar manner to that observed with Sigma 204 (Table 4-4). Conversely, Sigma antifoams O-30 and SE-15 did not appear to have any impact on either methanol or ammonium uptake Out of the two antifoams that were not inhibitory, only Sigma SE-15 was tested for its ability to reduce foam in a bioreactor, and it was effective. Hence Sigma SE-15 was selected as the antifoam agent in further high cell density cultivation studies.

**Table 4-4: Effect of different antifoams on methanol and ammonium uptake**

	Antifoam concentration (% v/v)	Methanol Utilized (%)	NH4 Utilized (%)
Control	0	73.6	73.7
Sigma SE-15	0.05	69.7	70.9
	0.1	72.3	71.1
	0.2	75.0	76.7
Sigma O-30	0.05	71.4	71.1
	0.1	71.0	76.0
	0.2	70.5	71.1
Canola vegetable oil	0.05	43.1	16.3
	0.1	26.0	2.0
	0.2	25.8	8.6

#### **4.2.2 Bioreactor studies: medium optimization**

Due to the intensive labor involved with carrying out yield and toxicity studies on all nutrients in the Higgin's growth medium (Cornish et al., 1984), particularly nutrients with an initial concentration less than 100 ppm, a fed-batch cultivation experiment, Fermentation 1 was carried out to determine the concentration profile of nutrients over the course of the fermentation. Methanol feeding commenced once the initial methanol concentration dropped to 1.4 g/L. The biomass, CCP and CMC profiles had a similar trend (Figure 4-5). The initial yield of carbon dioxide to methanol was 1.8 g/g which declined to approximately 0.8 g/g for the most part of the fermentation (Figure 4-5). All other growth nutrients were fed in excess over the course of the fermentation, the concentration profile of nutrients is shown in (Appendix C). The growth rates achieved were 0.013- 0.065 h<sup>-1</sup> (Table 4-5), which is slightly lower than growth rates on methanol 0.063-0.086 h<sup>-1</sup> reported by Best and Higgins (1981) and on methane 0.08 h<sup>-1</sup> (Mehta et al., 1989; Park et al., 1991). The method of estimating the growth rates in the current fed-batch study is outlined in Appendix D. The sMMO activity (315 -502 [ $\mu$ mol naphthol][g of biomass]<sup>-1</sup>[h]<sup>-1</sup>) is comparable to values that have been reported elsewhere (Bowman and Sayler, 1994). The overall yields of biomass to nutrients were estimated from the cumulative biomass produced and the cumulative nutrient consumption (Appendix E). A comparison of biomass yields to values from other studies is shown in Table 4-6. The methanol yield in this study (0.3 g dry cell wt/g CH<sub>3</sub>OH) is similar to those achieved in studies by Best and Higgins (1981) and Fitch et al., (1996). The yield from nitrogen

(ammonium source), 0.012 g dry cell wt/g N is also comparable to the value previously obtained 0.007 g dry cell wt/g N (nitrate source) by Park et al., (1991).

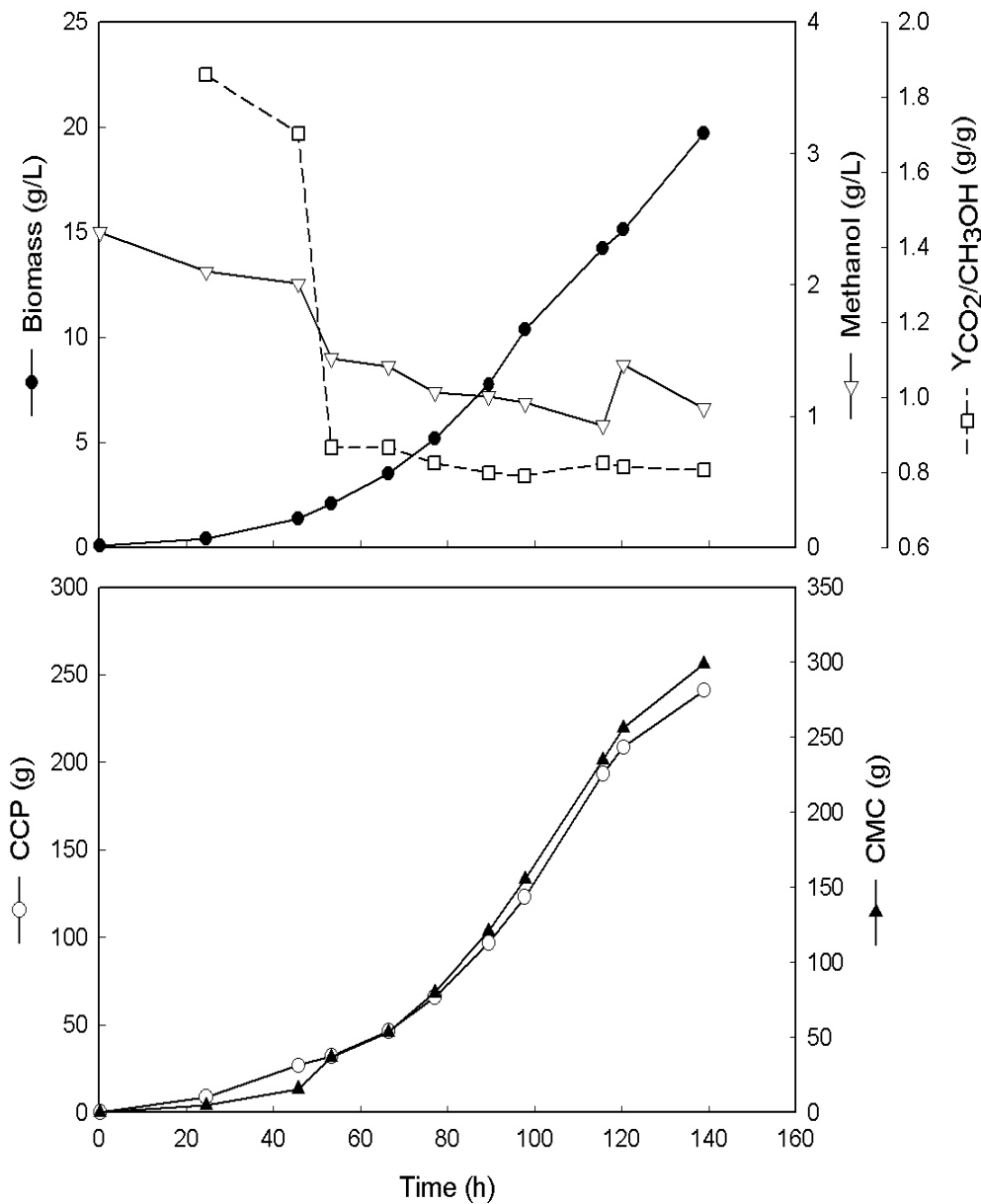


**Figure 4-5: Fermentation 1: Biomass, methanol, CCP, CMC and  $Y_{CO_2/CH_3OH}$  profiles.**

**CCP = cumulative carbon dioxide production.**

**CMC = cumulative methanol consumed.**

**$Y_{CO_2/CH_3OH}$  = yield of carbon dioxide to methanol**

**Table 4-5: Fermentation 1: Growth and sMMO production summary**

Total Biomass (g/L)	Growth rate (1/h)	Overall biomass productivity (g/L-h)	sMMO activity at 77 h [ $\mu$ moles naphthol].[g biomass -hr] <sup>-1</sup>	sMMO activity at 90 h [ $\mu$ moles naphthol].[g biomass -hr] <sup>-1</sup>
19.7	0.013- 0.065	0.14	315	502

**Table 4-6: Biomass yields of *Methylosinus trichosporium OB3b* on nutrients**

Nutrient	Yield biomass/nutrient (g/mg)				
	This study	Best and Higgins	Mehta et al	Fitch et al <sup>a</sup>	Park et al
Ca <sup>2+</sup>	2.47	-	-	-	-
Co <sup>2+</sup>	305	-	-	-	-
Fe <sup>2+</sup>	2.05	-	-	-	1.3
K <sup>2+</sup>	0.12	-	-	-	-
Mg <sup>2+</sup>	0.97	-	-	-	-
Mn <sup>2+</sup>	56.5	-	-	-	-
Na <sup>2+</sup>	0.14	-	-	-	-
Zn <sup>2+</sup>	39.2	-	-	-	-
PO <sub>4</sub> <sup>2-</sup>	0.03	-	-	-	-
Nitrogen	0.012 <sup>b</sup>	-	-	-	0.007 <sup>c</sup>
CH <sub>3</sub> OH (g/g)	0.3 ( $\pm$ 0.02)	0.4	-	0.4 ( $\pm$ 0.08)	-
CH <sub>4</sub> (g/g)	-	-	0.29	-	-

a: *Methylosinus trichosporium PP358* mutant strain.

b: Ammonium sulfate as nitrogen source

c: sodium nitrate as nitrogen source

#### **4.2.3 High cell density fed-batch cultivation (Fermentation 2)**

A fed-batch bioreactor study Fermentation 2, was carried out with medium B to achieve high cell density. The trace nutrients in Medium B were mixed together in a concentrated solution (Table 4-7) and fed according to the estimated methanol consumption. The estimation of the biomass yields from the nutrients in Fermentation 1 facilitated the design of a trace nutrients feeding strategy based on the amount of each nutrient required for a corresponding amount of methanol. The estimated amount of each trace nutrient utilized ( $M_i$ ) was determined online based on the amount of methanol consumed. Equation 4-4 shows the online calculation of consumed  $\text{Fe}^{2+}$ . The amount of each nutrient fed was then kept equal to  $M_i$  (Figure 4-6). Phosphate was fed manually based on the biomass yield. The initial methanol concentration in the bioreactor was 2g/L. Since higher growth rates were achieved at low methanol concentrations (Figure 4-3), feeding began once the initial methanol concentration decreased to 0.4 g/L. Sigma SE-15 was used as the antifoam agent.

$$M_{\text{Fe}^{2+}} = \text{CMC} \times Y_{\text{Fe}^{2+}/\text{CH}_3\text{OH}} \quad (\text{Equation 4-4})$$

Where  $M_{\text{Fe}^{2+}}$  is the estimated total amount of  $\text{Fe}^{2+}$  (g) consumed, CMC (g) is the cumulative methanol utilized and  $Y_{\text{Fe}^{2+}/\text{CH}_3\text{OH}}$  (g/g) is the yield of  $\text{Fe}^{2+}$  to methanol.

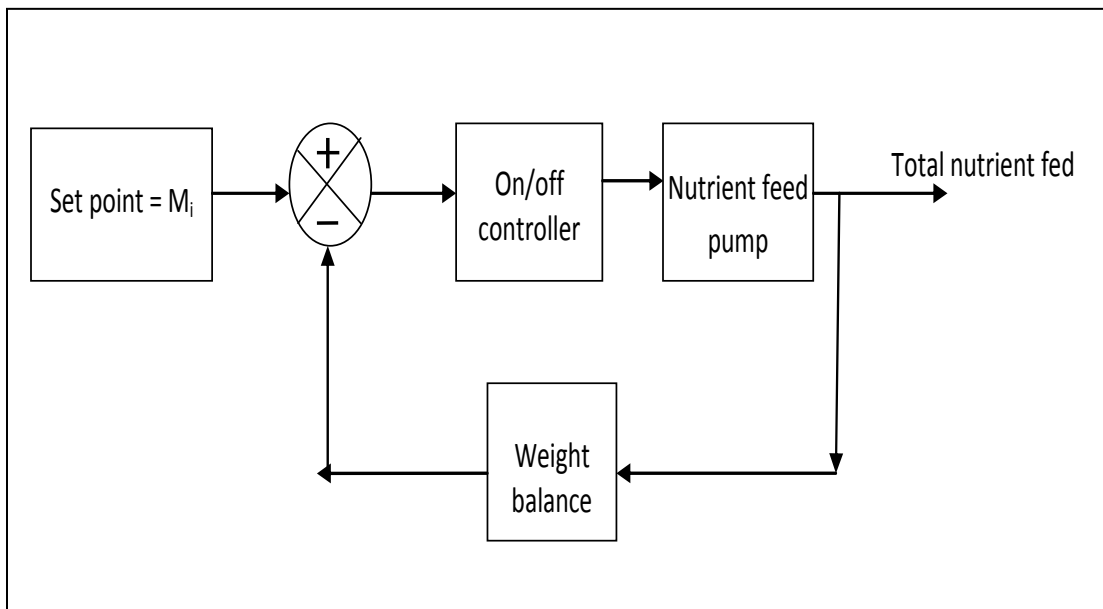


**Figure 4-6: Trace nutrients feeding strategy:**  $M_i$  = estimated nutrient consumed. The trace nutrient feed pump is on when the total nutrient fed is less than  $M_i$ .

**Table 4-7: Concentrated trace nutrient feed solution**

Trace nutrients	Concentration (g/L)
CaCl <sub>2</sub> .2 H <sub>2</sub> O	1.25
MgSO <sub>4</sub> .7 H <sub>2</sub> O	8.80
Fe SO <sub>4</sub> .7 H <sub>2</sub> O	2.04
ZnSO <sub>4</sub> .7 H <sub>2</sub> O	0.09
MnSO <sub>4</sub> .7H <sub>2</sub> O	0.07
H <sub>3</sub> BO <sub>3</sub>	0.02
NaMoO <sub>4</sub> .2H <sub>2</sub> O	0.24
COCl <sub>2</sub> .6H <sub>2</sub> O	0.01
KI	0.03

During the early growth phase, cells of *M. trichosporium OB3b* have a high demand for CO<sub>2</sub>. Therefore CO<sub>2</sub> (3.5 ± 0.05%) was supplied in the air stream to the bioreactor. However in the exponential growth phase, similar growth rates were observed in batch cultures grown with and without external CO<sub>2</sub> supply (Park et al., 1991). In that study, biomass growth was in the exponential phase at a cell density of approximately 0.3 g/L, hence in this study the supplemental CO<sub>2</sub> was discontinued once the biomass exceeded 1g/L.

Biomass, CCP and CMC profiles from Fermentation 2 are shown in Figure 4-7. Approximately 62 g/L of biomass was produced. This is the highest cell density ever reported for the cultivation of *M. trichosporium OB3b*. The previous highest biomass density was 18 g/L by Shah et al., (1996). Biomass productivity, 0.44 g/L-h was three times higher in Fermentation 2 (Table 4-5 and 4-8), indicating a significant improvement in cultivation conditions. Methanol in Fermentation 1 was controlled at 1.4 g/L and at 0.4 g/L in Fermentation 2, thus a weaker methanol inhibitory effect may have contributed to the improved biomass productivity. The overall biomass yield from methanol was 0.32 g/g. The sMMO activity, 8.6 [μmol naphthol][g of biomass]<sup>-1</sup>[h]<sup>-1</sup> was much lower in Fermentation 2 because the inoculum had lost the ability to produce high levels of sMMO. Chapter 5 focuses on efforts to recover sMMO activity.

The Y<sub>CO<sub>2</sub>/CH<sub>3</sub>OH</sub> was calculated by online measurement of CCP and CMC. It was adjusted automatically (every 15 min) over the course of the fed-batch cultivation. The apparent yield (2 ± 0.25 g/g or 1.45 ± 0.18 mol/mol) was higher at the earlier stages of

the fed-batch cultivation experiments (Figure 4-5 and 4-7). This range exceeds the maximum possible yield which is 1 mol/mol assuming all methanol is converted to carbon dioxide. This indicates an error in the estimation of the initial apparent yield. In the early growth phase, the supplementation of  $3.5 \pm 0.5\%$  CO<sub>2</sub> probably resulted in an overestimation of the initial CCP used in calculating the apparent yield. As growth continued and CO<sub>2</sub> production rate increased, this error became negligible. Hence the ability to fine tune the apparent Y<sub>CO<sub>2</sub>/CH<sub>3</sub>OH</sub> online proved crucial particularly during the early growth phase. The CCP feeding strategy with online yield estimation precluded the overfeeding of methanol to the bioreactor. Therefore the fail-safe methanol feedback control was not executed.

**Table 4-8: Fermentation 2: Growth and sMMO production summary**

Total Biomass (g/L)	Growth rate (1/h)	Overall biomass productivity (g/L-h)	sMMO activity at 41 h [ $\mu$ moles naphthol].[g biomass -hr] <sup>-1</sup>	sMMO activity at 143 h [ $\mu$ moles naphthol].[g biomass -hr] <sup>-1</sup>
62.8	0.034- 0.080	0.44	9.3	8.6

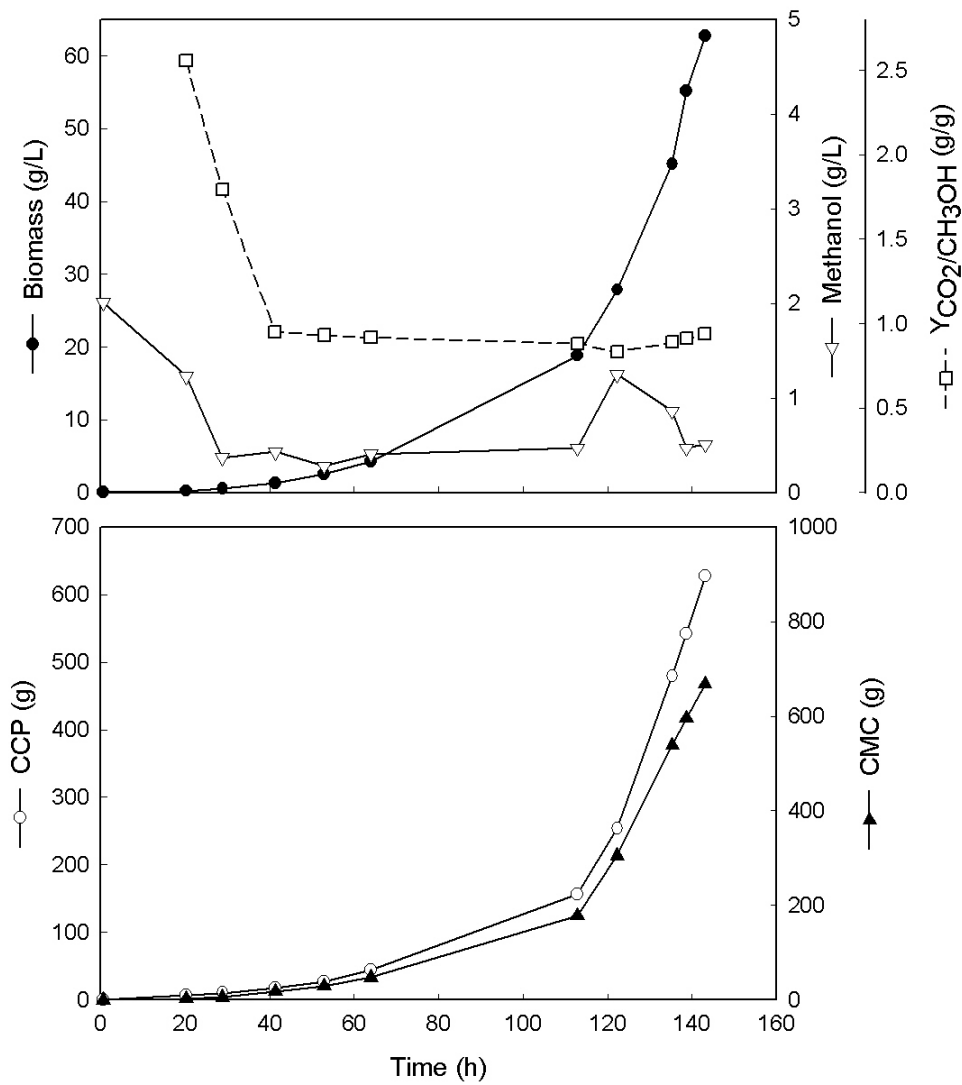


**Figure 4-7: Fermentation 2: Biomass, methanol,  $Y_{CO_2/CH_3OH}$ , CCP and CMC profiles.**

The growth rates were higher during the initial (0-65 h) phase of growth ( $0.05 - 0.08 \text{ h}^{-1}$ ). However the growth rate declined to  $0.036 \pm 0.02 \text{ h}^{-1}$  in the later growth phase ( $> 65 \text{ h}$ ). It is probable that the decrease in growth rate was due to ammonium inhibition. The automatic feeding of trace nutrients which were dissolved in an acidic solution (pH

3.0) began at 54 h. This caused a decrease in the overall pH of the growth medium and an increase in the ammonium hydroxide added to control pH. Ammonium concentration in the bioreactor increased (Figure 4-8) which subsequently had an adverse effect on cell growth rates (Figure 4-9).

The fed-batch cultivation terminated due to excessive foaming caused by phosphate limitation. At approximately 120 h, the phosphate concentration dropped below optimal concentration for growth, 0.19 g/L (2mM) and continued to decline thereafter (Figure 4-8). The phosphate limitation was a result of operator error in phosphate feeding. The low phosphate concentration caused a reduction in buffering capacity. This may have contributed to the increased ammonium feeding. Maintaining the initial phosphate concentration over the course of the fermentation and using a less acidic trace nutrient solution would prevent ammonium overfeeding.

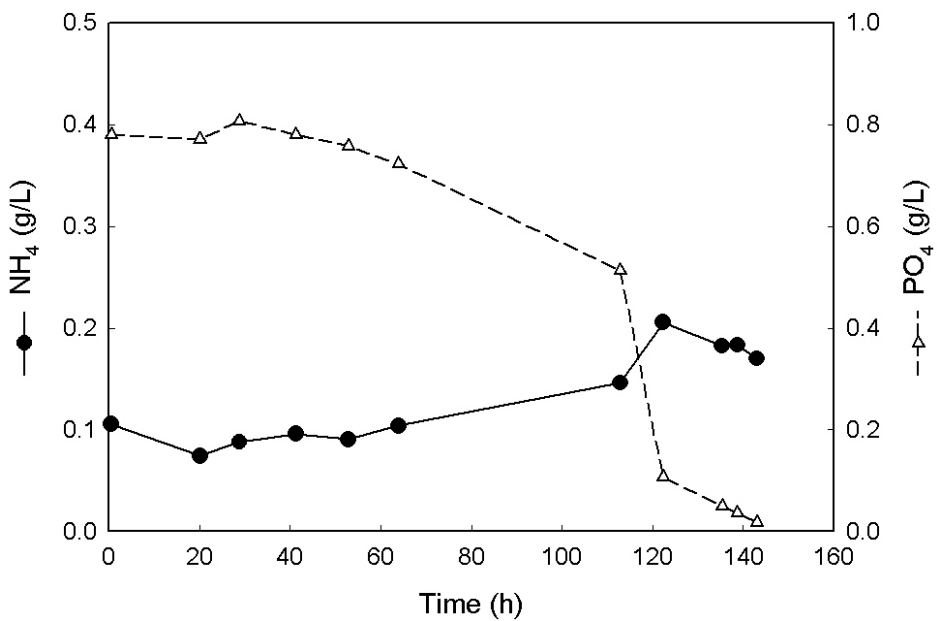


**Figure 4-8: Ammonium and phosphate concentration profiles.**

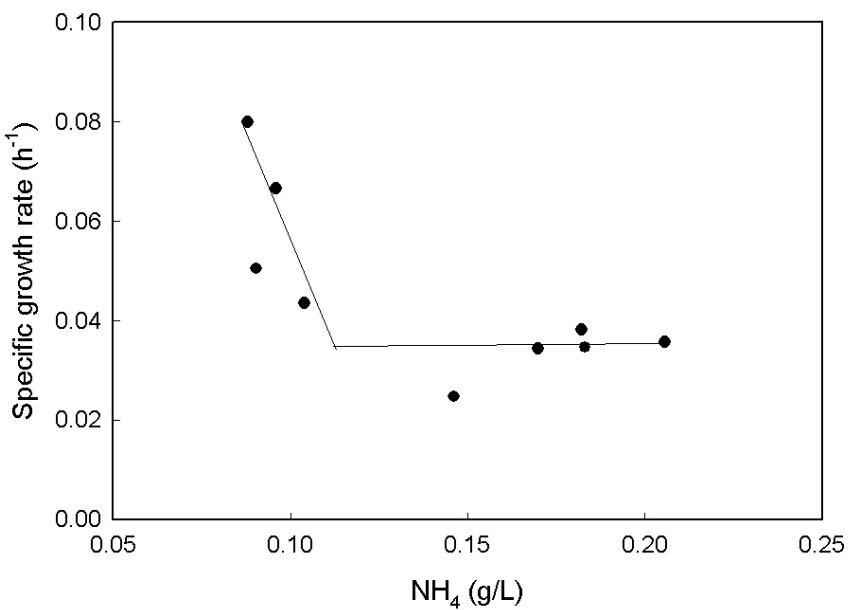


**Figure 4-9: Fermentation 2: Effect of ammonium on growth rate.**

### **4.3 Conclusions**

The ability to perform online measurements on both carbon dioxide production and the mass of total substrate fed, provided a means of executing the CCP feeding strategy. Since methanol is an inhibitory substrate, the ability to measure methanol concentration online was beneficial in fine-tuning values of  $Y_{CO_2/CH_3OH}$  utilized in the feeding strategy which maintained an almost constant methanol concentration. The overall yield of CO<sub>2</sub> from methanol was 0.94 g/g. The studies carried out on inhibitory effects of methanol and ammonium showed that concentrations below 2 g/L and 0.09 g/L (5 mM) respectively were most favorable for rapid growth. The cell yield from methanol and nitrogen were estimated to be 0.3 g dry cell wt/g CH<sub>3</sub>OH and 12 g dry cell wt/g N respectively. It was shown that it is possible to cultivate *M. trichosporium OB3b* on methanol while retaining high sMMO activity (300 -500 [ $\mu$ mol naphthalol][g of biomass]<sup>-1</sup>[h]<sup>-1</sup>). The estimation of yield parameters provided a basis of modifying the Higgin's NMS medium (Cornish et al., 1984). This facilitated the automatic feeding of nutrient salts based on their yields to methanol in fed-batch reactor runs. Sigma 204 and canola vegetable oil were inhibitory antifoam agents. Sigma SE-15 was not inhibitory to growth and was effective in reducing foaming. As a result of an improved trace nutrient feeding strategy and operation at a low methanol concentration (0.4 g/L), final biomass density of 62 g/L and productivity of 0.44 g/L-h were achieved.

## **Chapter 5**

### **Recovering sMMO activity**

After 6 months of cultivation on NMS Noble agar with methane, the sMMO activity of *M. trichosporium OB3b* decreased from ~500 to less than 80  $\mu\text{mol}$   $\mu\text{mol}$  [naphthol][g of biomass] $^{-1}[\text{h}]^1$ . The copper concentration in the growth medium B (Table 4-1) was found to be less than 0.01 ppm which should favor sMMO production. Hence, the effect of a pMMO inhibitor (allylthiourea) on sMMO activity was investigated. In addition, the effect of nitrogen source on sMMO activity was studied.

#### **5.1 Materials and methods**

Cultures were cultivated in shake flasks and incubated at 30°C and 200 rpm in an incubator shaker (Innova 44, New Brunswick Scientific, Edison, NJ USA). The inoculum for each shake flask study was prepared from plate cultures. The sMMO activity was analyzed by the naphthalene oxidation method (Brusseau et al., 1990; Tsien et al., 1989). Biomass samples were centrifuged (10,000 xg for 10 min) and resuspended in medium C to a cell density of 0.5g/L. Potassium formate (20 mM) was added to serve as an energy source. The samples were then incubated with excess naphthalene crystals at 30°C and 200 rpm for 1 h. The incubated solution was then centrifuged (10,000 xg for 10 min) and the supernatant was tested for naphthol by reaction with 0.1 mL of tetrazotized o-dianisidine to form a purple diazo dye. The mixture was stabilized with 0.4 mL acetic acid. The absorbance was measured within 15 min at a wavelength of 530 nm and

correlated to naphthol concentration via a calibration curve freshly prepared with 0 to 7 mg/L 1-naphthol.

## 5.2 Results and discussion

### 5.2.1 Effect of nitrogen source on sMMO activity

The sMMO activity of ammonium-grown cells was compared to that of nitrate-grown cells. An inoculum which was prepared on methanol (2 g/l) and medium B (Table 4-1) was centrifuged and rinsed 3 times in phosphate buffer solution prior to being used to inoculate 2 sets of triplicate shake flasks. The first set of flasks were cultivated with ammonium sulfate as the nitrogen source (7.6 mM nitrogen), while the second set was cultivated with sodium nitrate (7.6 mM nitrogen). The enzyme activity in each flask was measured after 4 days of growth.

Since ammonium competes with methane for the active site on sMMO (King and Schnell 1994; Whittenbury et al., 1970), it was expected that cells cultivated with ammonium would have lower sMMO activity. However, there was no significant difference (ANOVA) in sMMO activity of ammonium and nitrate grown cells (Table 5-1), indicating that ammonium (7.6 mM) does not inhibit sMMO production, although it may compete with methane for the sMMO active site.

**Table 5-1: Effect of equimolar concentration of ammonium and nitrate on sMMO activity**

Nitrogen source (7.6 mM)	sMMO activity ( $\mu$ moles naphthol/g biomass -hr)
nitrate	17.1 $\pm$ 2.8
ammonium	18.4 $\pm$ 2.0

Nitrate was supplied as sodium nitrate and ammonium from ammonium sulfate

### 5.2.2 Effect of allylthiourea on sMMO recovery

Two experiments were carried out: The first involved two sets of methanol-grown cells (4 g/L) in triplicate, cultivated in NMS medium B with and without allylthiourea. The second set of experiments (in duplicate), was identical to the first except the cells were cultivated on methane which was replenished daily with a methane/air mixture (4:1) at a flow rate of 3 L/min for 5 min. The inocula for each group of experiments were prepared with medium B and 2 g/L methanol.

Allylthiourea acts as a copper chelator (Hubley et al., 1975), limiting cell access to copper and thus promoting the switch from pMMO to sMMO production. Therefore, the addition of allylthiourea to the growth medium should sequester the available copper and increase sMMO production. In the methanol cultures, sMMO activity is about two orders of magnitude lower than the nominal range of 300 to 600 [ $\mu$ mol naphthol][g of biomass]<sup>-1</sup>[h]<sup>-1</sup>. There was no significant impact of 15  $\mu$ M allylthiourea on enzyme activity in methanol grown cells (Table 5-2). However with the methane grown cells, the enzyme activity was higher for both set of cultures. It is probable that for the cultures

growing on methanol, there was little driving force to stimulate the production of sMMO because it is not required by the cells for methanol metabolism. However in the methane-cultivated cells, the enzyme is necessary for methane metabolism, thus the cells had to produce sMMO for survival. The methane grown cultures without allylthiourea had higher biomass density and sMMO activity than cells grown in medium containing 15  $\mu\text{M}$  allylthiourea. The copper content in medium B was less than 0.01 ppm, since allylthiourea is a metal chelator, with an affinity for ions with a 2+ charge, it is likely that with such a low  $\text{Cu}^{2+}$  concentration in the growth medium, allylthiourea may have sequestered another cation such as  $\text{Fe}^{2+}$  which is required for sMMO production.  $\text{Fe}^{2+}$  has been shown by Shah et al., (1992) to be required for high levels of sMMO synthesis. Therefore allylthiourea was not necessary to promote sMMO production since there was a low level of copper in the growth medium.

**Table 5-2: Effect of allylthiourea on methanol and methane grown cells**

Carbon source	ATU ( $\mu\text{M}$ )	Final biomass (g/L)	sMMO activity [ $\mu\text{ moles naphthol}].[\text{g biomass -hr}]^{-1}$	Average % increase in sMMO activity compared with inoculum
Methanol	0	$1.02 \pm 0.02$	$8.61 \pm 1.04$	104
	15	$1.02 \pm 0.01$	$9.67 \pm 0.49$	129
Methane	0	$0.58 \pm 0.2$	$63.8 \pm 28.4$	1858
	15	$0.12 \pm 0.01$	$23.4 \pm 7.4$	617

### **5.2.3 Effect of methane on sMMO activity of methanol grown cells**

To investigate the effect of methane exposure to methanol grown cells, a biomass sample containing 62 g/L *M. trichosporium OB3b* obtained from a methanol fed-batch bioreactor (Fermentation 2) was resuspended (0.67% v/v) in NMS medium C (Table 4-1) containing 15 $\mu$ M allylthiourea and cultivated for a week before being subcultured (33% v/v) into a similar medium and grown for four days. Methane was utilized as the sole carbon source in this experiment and was fed along with air (4:1) to the shake flasks daily at a flow rate of 3 L/min.

The enzyme activity increased 70- fold when cells obtained from the bioreactor were subcultured on methane (Figure 5-1). A similar phenomenon was observed in the allylthiourea experiment (Table 5-2), in which the inocula were grown on methanol. It appears that methane induces the production of high levels of sMMO. Thus it is advantageous to first cultivate *M. trichosporium OB3b* on methanol in a liquid medium to obtain rapid growth to a sufficient biomass density and then switching the sole source of carbon to methane. In copper free media, at high cell densities, there is an increased competition for the carbon source, methane which stimulates the cells to produce more sMMO for survival.

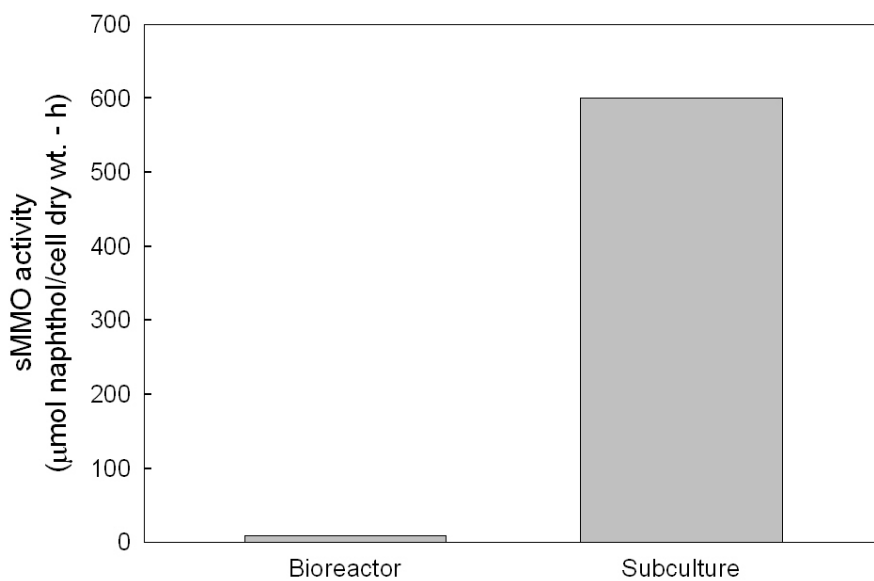


**Figure 5-1: Recovery of sMMO activity in subcultures grown on methane.**

### **5.3 Conclusions**

There was no significant effect of ammonium (7.6 mM) on the sMMO activity of methanol grown cultures of *M. trichosporium OB3b*. Attempts to promote sMMO production by the addition of allylthiourea (15 µM) to the growth medium failed. In low-copper containing media (< 0.01 ppm), it is probable that allylthiourea may sequester other cations such as Fe<sup>2+</sup> that are required for sMMO production. Allylthiourea is not necessary to promote whole cell sMMO activity of cells grown under copper stress. However sMMO activity can be recovered in *M. trichosporium OB3b* by cultivating in a copper-free liquid NMS medium with methane (in excess) as the sole carbon source.

## **Chapter 6**

### **Conclusions**

The use of the probe equipped with the Figaro TGS 822 sensor for online methanol measurement was effective for fed-batch cultivation. The long response time (12 min) of the probe can be improved upon by increasing the gas permeability of the membrane. The probe provided a means of fine-tuning the yield of CO<sub>2</sub> from methanol online, which was used in the CCP strategy for methanol feeding. The CCP strategy was effective at providing an adaptive control of methanol concentration. Ammonium was inhibitory at concentrations exceeding 5 mM (0.09 g/L). Antifoaming agent, Sigma SE-15 had no effect on cell growth while vegetable oil and Sigma antifoam 204 were inhibitory. The nutrient yields in the Higgin's NMS growth medium (Cornish et al., 1984) were determined, and a growth medium B was designed based on yield ratios.

The automatic feeding of methanol along with other growth nutrients (according to nutrient yields on methanol) was vital in producing a high cell density of 62 g/L which is the highest reported in literature. The fermentation stopped due to an operator error in phosphate feeding which resulted in excessive foaming. Perhaps, it would have been possible to achieve much higher biomass densities if the error was precluded. The yields and nutrient inhibition data obtained in this study will be useful for large scale biomass production applications (e.g. bioremediation).

It was shown that *M. trichosporium* OB3b can be cultivated on methanol while retaining high sMMO activity (300-500 [μmol naphthol][g of biomass]<sup>-1</sup>[h]<sup>-1</sup>).

Subcultivation in a copper-free liquid NMS medium with methane as the sole carbon source is an effective method to recover whole cell enzyme activity in cultures of *M. trichosporium* OB3b expressing low sMMO.

## **Chapter 7** **Recommendations and future work**

*M. trichosporium OB3b* has a high potential in the bioremediation industry due to its ability to degrade ubiquitous groundwater contaminants such as trichloroethylene. Perhaps, the most practical application involves a pump and treat system, where contaminated groundwater is slowly pumped into a bioreactor (or multiple reactors in series) inoculated with high cell densities of *M. trichosporium OB3b* (with high sMMO activity).

To make the application (e.g. epoxide production) of *M. trichosporium OB3b* more commercially feasible, higher biomass productivity is required. It is recommended that further work be carried out on achieving higher growth rates on methanol. The maximum growth rate on methanol can be determined through chemostat studies.

For bioremediation and other applications of sMMO, further studies on the mechanism of methane monooxygenase production may conceivably provide insights which will allow for better manipulation of culture environment to stimulate higher sMMO production in methanol grown cultures.

## Bibliography

- Anderson, J.E. and McCarty, P.L. 1996. Effect of Three Chlorinated Ethenes on Growth rates for a Methanotrophic Mixed Culture. *Environ. Sci. Technol.* 30 (12): 3517-3524
- Anthony, C. 1982. The biochemistry of methylotrophs. Academic Press. London
- Bielefeldt, A.R., Stensel, H.D., and Strand, S.E. 1994. Degradation of chlorinated aliphatic compounds by methane and phenol-oxidizing Bacteria. In: Bioremediation of chlorinated solvents. pp. 237-244. (Hinchee, R.E., Leeson, A., and Semprini,). Battelle Press: Columbus, Ohio.
- Best, D.J. and Higgins, I.J. 1981. Methane-oxidizing activity and membrane morphology in a methanol-grown obligate methanotroph, *Methylosinus trichosporium OB3b*. *Gen. Microbiol.* 125 (1): 73 -84.
- Bowman, J.P. and Sayler, G.S. 1994. Optimization and maintenance of soluble methane monooxygenase activity in *Methylosinus trichosporium OB3b*. *Biodegradation* 5 (1): 1-11.
- Brusseau, G.A., Tsien, H.C., Hanson, R.C., and Wackett, S.P. 1990. Optimization of trichloroethylene oxidation by methanotrophs and the use of a colorimetric assay to detect soluble methane monooxygenase activity. *Biodegradation* 1 (1): 19-29.
- Canadian Council of Ministers of the Environment. 2006. Canada: CCME.
- Cardinal, L., and Stenstrom, M. 1991. Enhanced biodegradation of polyaromatic hydrocarbons in the activated sludge process. *Res. J. WPCF.* 63: 950-957
- Chen, Y. 1988. Reconstitution of the electron-transport system that couples formate oxidation to nitrogenase in *Methylosinus trichosporium OB3b*. *Gen. Microbiol.* 134 (12): 3123-3128.
- Chen, Y. and Yoch, D.C. 1987. Regulation of 2 nickel-requiring (inducible and constitutive) hydrogenases and their coupling to nitrogenase in *Methylosinus trichosporium OB3b*. *J. Bact.* 169 (10): 4778-4783.
- Chu, H. and Alvarez-Cohen, L. 1998. Effect of nitrogen source on growth and trichloroethylene degradation by methane-oxidizing bacteria. *Appl. Environ. Microbiol.* 64 (9): 3451-3457.
- Colby, J., Stirling, D.I. and Dalton, H. 1977. The soluble methane mono-oxygenase of *Methylococcus capsulatus (bath)*, its ability to oxygenate n-alkanes, n-alkenes,

- ethers, and alicyclic, aromatic and heterocyclic compounds. *Biochem* 165 (2): 395-402.
- Cornish, A., Nicholls, K.M., Scott, D., Hunter, B.K., Aston, W.J., Higgins, I.J., and Sanders, J.K.M. 1984. *In vivo* C-13 nmr investigations of methanol oxidation by the obligate methanotroph *Methylosinus trichosporium OB3b*. *Gen. Microbiol.* 130 (10): 2565-2575.
- Dalton, H., Golding, B., and Waters, B. 1981. Oxidation of cyclopropane, methylcyclopropane, and arenes with the monooxygenase system from *Methylococcus capsulatus* (bath). *J. C. S. Chem. Commun.* 189: 482-483
- Davis, K., Cornish, A., and Higgins, I.J. 1987. Regulation of the intracellular location of the methane mono-oxygenase during growth *Methylosinus trichosporium OB3b* on methanol. *Gen. Microbiol.* 133 (2): 291-297.
- DiSpirito, A.A., Gullede, J., Shiemke, A.K., Murrell, J.C., Lidstrom, M.E., and Krema, C.L. 1991. Trichloroethylene oxidation by the membrane-associated methane monooxygenase in type I, type II and type X methanotrophs. *Biodegradation* 2 (3): 151-164.
- Figaro Engineering Inc. 2004. General information for TGS sensors.
- Fitch, M.W., Speitel, J., and Georgiou, G. 1996. Degradation of trichloroethylene by methanol-grown cultures of *Methylosinus trichosporium OB3b PP358*. *Appl. Environ. Microbiol.* 62 (3): 1124-1128.
- Fox, B.G., Froland, W.A., Dege, J.E., and Lipscomb, J.D. 1989. Methane monooxygenase from *Methylosinus trichosporium OB3b*, purification and properties of a three-component system with high specific activity from a type II methanotroph. *J. Biol. Chem.* 264 (17): 10023-1033.
- Fox, B., Bourneman, J., Wackett, L., and Lipscomb, J. 1990. Haloalkene oxidation by the soluble methane monooxygenase from *Methylosinus trichosporium OB3b*: mechanistic and environmental implications. *Biochem.* 29: 6419-6427
- Guarna, M.M., Lesnicki, G.J., Tam, B.M., Robinson, J., Radziminski, C.Z., Hasenwinkle, and D., Boraston, A. 1997. On-line monitoring and control of methanol concentration in shake-flask cultures of *Pichia pastoris*. *Biotechnol. Bioeng.* 56 (3): 279-286.
- Hanson, R.S., and Hanson, T.E. 1996. Methanotrophic bacteria. *Microbiol Rev.* 60 (2): 439-471.

- Heiland, G. 1982. Homogeneous semiconducting gas sensors. *Sensors Actuators*, 2 (4): 343-361.
- Hubley, J.H., Thomson, A.W., and Wilkinson, J.F. 1975. Specific inhibitors of methane oxidation in *Methylosinus trichosporium*. *Arch. Microbiol.* 102 (3): 199-202.
- Jahng, D., and Wood, T.K. 1996. Metal ions and chloramphenicol inhibition of soluble methane monooxygenase from *Methylosinus trichosporium OB3b*. *Appl. Microbiol. Biotechnol.* 45 (6): 744.
- Jensen, S., Prieme, A., and Bakken, L. 1998. Methanol improves methane uptake in starved methanotrophic microorganisms. *Appl. Environ. Microbiol.* 64 (3): 1143-1146.
- Jollie, D.R., and Lipscomb, J.D. 1991. Formate dehydrogenase from *Methylosinus trichosporium OB3b* – Purification and spectroscopic characterization of the cofactors. *J. Biol. Chem.* 266 (32): 21853-21863.
- Jones, T.A., Firth, J.G., and Mann, B. 1985. The effect of oxygen on the electrical conductivity of some metal oxides in inert and reducing atmospheres at high temperature. *Sensors Actuators*. 8 (4): 281-306.
- Katakura, Y. 1998. Effect of methanol concentration on the production of human β2-glycoprotein I domain V by a recombinant *Pichia pastoris*: A simple system for the control of methanol concentration using a semiconductor gas sensor. *J. Ferment. Bioeng.* 86 (5): 482-487.
- Keenan, J.E., Strand, S.E., and Stensel H.D. 1994. Degradation kinetics of chlorinated solvents by a propane-oxidizing enrichment culture. In: Bioremediation of chlorinated and polycyclic aromatic hydrocarbon compounds. pp. 1-13. (Hinchee, R.E., Leeson, A., Semprini, L. and Ong, S.K.). Lewis Publishers: Boca Raton, Florida.
- Kim, P., Kim, J., and Oh, D. 2003. Improvement in cell yield of *Methylobacterium sp* by reducing the inhibition of medium components for poly-beta-hydroxybutyrate production. *World. J. Microbiol. Biotechnol.* 19 (4): 357-361.
- King, G.M., and Schnell, S. 1994. Ammonium and nitrite inhibition of methane oxidation by *Methylobacter albus BG8* and *Methylosinus trichosporium OB3b* at low methane concentrations. *Appl. Environ. Microbiol.* 60 (10): 3508-3513.
- Lanzetta, P.A., Alvarez, L.J., Reinach, P.S., and Candia, O.A. 1979. An improved assay for nanomole amounts of inorganic phosphate. *Anal. Biochem.* 100 (1): 95-97.

- Leak, D.J., and Dalton, H. 1986. Growth yields of methanotrophs. 2. A theoretical analysis. *Appl. Environ. Microbiol.* 23 (6): 477-481.
- Lee, J., Soni, B.K. and Kelley, R.L. 1996. Cell growth and oxygen transfer in *Methylosinus trichosporium OB3b* cultures. *Biotechnol. Lett.* 18 (8): 903-908.
- Lidstrom, M.E., and Stirling, D.I. 1990. Methylotrophs: Genetics and commercial applications. *Annu. Rev. Microbiol.* 44: 27-58.
- Lipscomb, J.D. 1994. Biochemistry of the soluble methane monooxygenase. *Annu. Rev. Microbiol.* 48: 371-399.
- Mehta, P.K., Mishra, S., and Ghose, T.K. 1987. Methanol accumulation by resting cells of *Methylosinus trichosporium* 1. *Gen. Appl. Microbiol.* 33 (3): 221-229.
- Mehta, P.K., Mishra, S., and Ghose, T.K. 1989. Growth kinetics and methanol oxidation in *Methylosinus trichosporium* NCIB 11131. *Biotechnol. Appl. Biochem.* 11 (3): 328-335.
- Morrison, S.R. 1982. Semiconductor gas sensors. *Sensors Actuators* 2 (4): 329-341.
- Morton, J.D., Hayes, K.F., and Semrau, J. 2000. Effect of copper speciation on whole-cell soluble methane monooxygenase activity in *Methylosinus trichosporium OB3b*. *Appl. Environ. Microbiol.* 66 (4): 1730-1733.
- Murrel, C.J. 1988. The rapid switch-off of nitrogenase activity in obligate methane-oxidizing bacteria. *Arch. Microbiol.* 150 (5): 489-495.
- Murrel, C.J., and Dalton, H. 1983. Nitrogen- fixation in obligate methanotrophs. *Gen. Microbiol.* 129 (11): 3481-3486.
- Noronha, S.B., Wagner, L.W., Matheson, N.H., and Shiloach, J. 1999. Use of an ethanol sensor for feedback control of growth and expression of TBV25H in *Saccharomyces cerevisiae*. *Biotechnol. Bioeng.* 63 (3): 285-289.
- Oldenhuis, R., Oedzes, J.Y., Van der Waarde, J.J., and Janssen, D.B. 1991. Kinetics of chlorinated hydrocarbon degradation by *Methylosinus trichosporium OB3b* and toxicity of trichloroethylene. *Appl. Environ. Microbiol.* 57 (1): 7-14.
- O'Neill, J.G., and Wilkinson, J.F. 1977. Oxidation of ammonia by methane-oxidizing bacteria and effects of ammonia on methane oxidation. *Gen. Microbiol.* 100 (2): 407-412.

- Park, S., Hanna, L.M., Taylor, R.T. and Droege, M.W. 1991. Batch cultivation of *Methylosinus trichosporium OB3b*. I: Production of soluble methane monooxygenase. *Biotechnol. Bioeng.* 38 (4): 423-433.
- Park, S., Shah, N.N., Taylor, R.T., and Droege, M.W. 1992. Batch cultivation of *Methylosinus trichosporium OB3b*: II. production of particulate methane monooxygenase. *Biotechnol.. Bioeng.* 40 (1):151-157.
- Ramon, R., Feliu, J.X., Cos, O., Montesinos, J.L., Berthet, F.X., and Valero, F. 2004. Improving the monitoring of methanol concentration during high cell density fermentation of *Pichia pastoris*. *Biotechnol. Lett.* 26 (18): 1447-1452.
- Shah, N.N., Park, S., Taylor, R.T., and Droege, M.W. 1992. Cultivation of *Methylosinus trichosporium OB3b*: III. production of particulate methane monooxygenase in continuous culture. *Biotechnol. Bioeng.* 40 (6): 705-712.
- Shah, N.N., Hanna, L.M., and Taylor, R.T. 1996. Batch cultivation of *Methylosinus trichosporium OB3b* .5. characterization of poly-beta-hydroxybutyrate production under methane-dependent growth conditions. *Biotechnol. Bioeng.* 49 (2): 161-171.
- Stanley, S.H., Prior, S.D., Leak, D.J., and Dalton, H. 1983. Copper stress underlies the fundamental change in intracellular location of methane mono-oxygenase in methane-oxidizing organisms - studies in batch and continuous cultures. *Biotechnol. Lett.* 5 (7): 487-492.
- Stephen, D., Prior, D., and Dalton, H. 1985. The effect of copper ions on membrane content and methane monooxygenase activity in methanol-grown cells of *Methylococcus capsulatus (bath)*. *Gen. Microbiol.* 131 (1): 155-163.
- Sullivan, J.P., Dickinson, D., and Chase, H.A. 1998. Methanotrophs, *Methylosinus trichosporium OB3b*, sMMO, and their application to bioremediation. *Crit. Rev. Microbiol.* 24 (4): 335-373.
- Tsien, H.C., Brusseau, G.A., Hanson, R.S., and Waclett, L.P. 1989. Biodegradation of trichloroethylene by *Methylosinus trichosporium OB3b*. *Appl. Environ. Microbiol.* 55 (12): 3155-3161.
- Wagner,L.W., Matheson,N.H., Heisey,R.F., and Schneider,K. 1997. Use of a silicone tubing sensor to control methanol concentration during fed batch fermentation of *Pichia pastoris*. *Biotechnol. Techniques.* 11 (11): 791-795.
- Watson,J. 1984. The tin oxide gas sensor and its applications. *Sensors Actuators.* 5 (1): 29.

Weatherburn,M.W. 1967. Phenol-hypochlorite reaction for determination of ammonia.  
*Anal. Chem.* 39 (8): 971-974.

Whittenbury, R., Phillips, K.C., and Wilkinson, J.F. 1970. Enrichment, isolation and  
some properties of methane-utilizing bacteria. *Gen. Microbiol.* 61 (2): 205-218.

Yoshinari, T. 1985. Nitrite and nitrous-oxide production by *Methylosinus trichosporium*.  
*Can. J. Microbiol.* 31 (2): 139-144.

## Appendix A Figaro Sensor

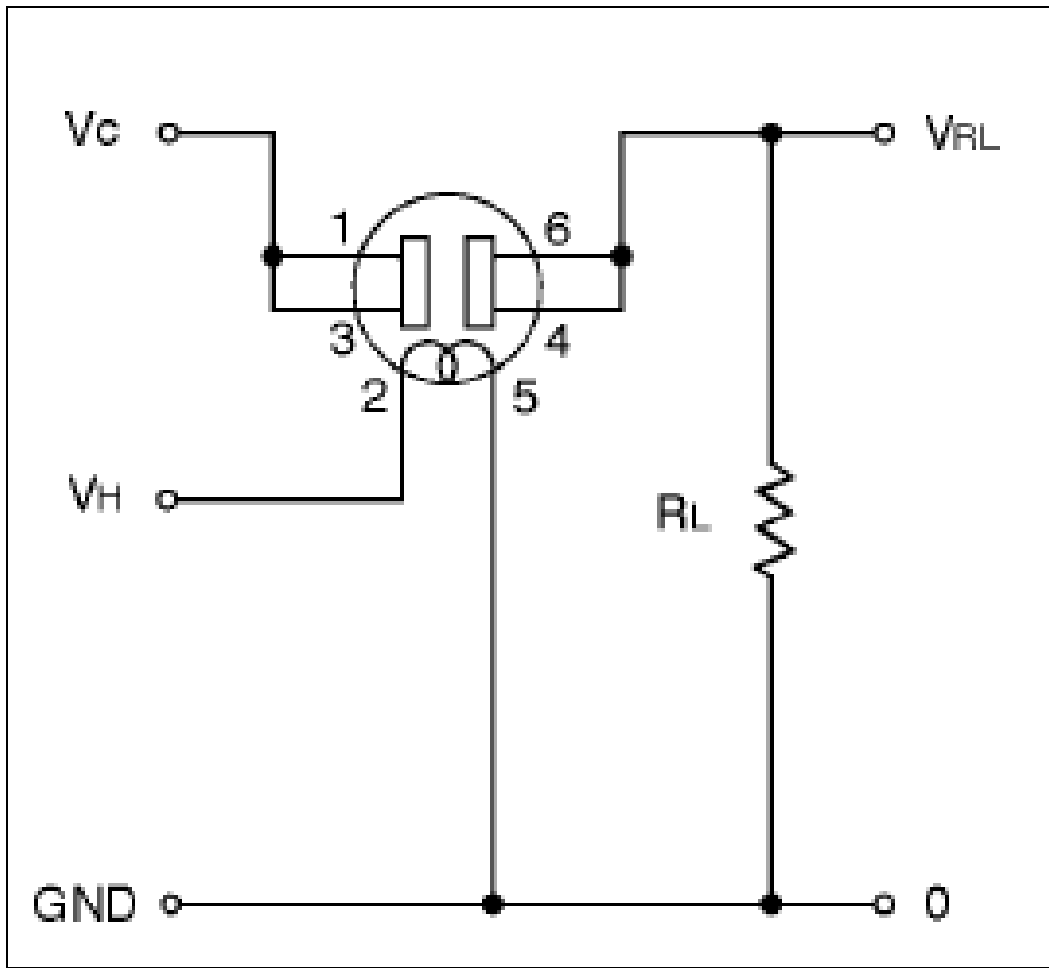
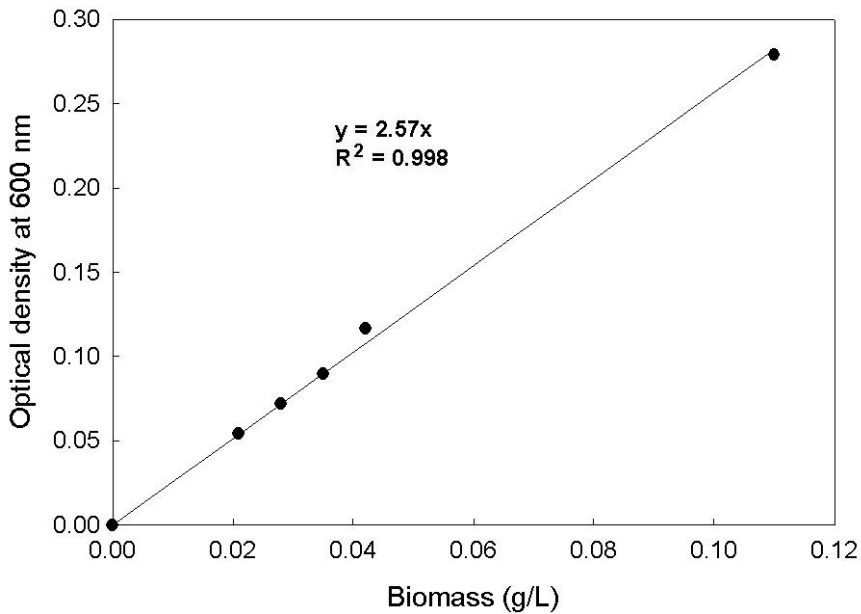


Figure A- 1: Circuit diagram for Figaro TGS 822 sensor: 5Volts is supplied to the circuit  $V_C$  and heater  $V_H$ . Once the circuit is connected,  $V_{RL}$  increases if gaseous methanol is introduced. A calibration can then be carried out to relate methanol concentration to  $V_{RL}$  (Figaro Engineering, 2004).

## **Appendix B**

### **Calibration curves**



**Figure B- 1: Biomass calibration**

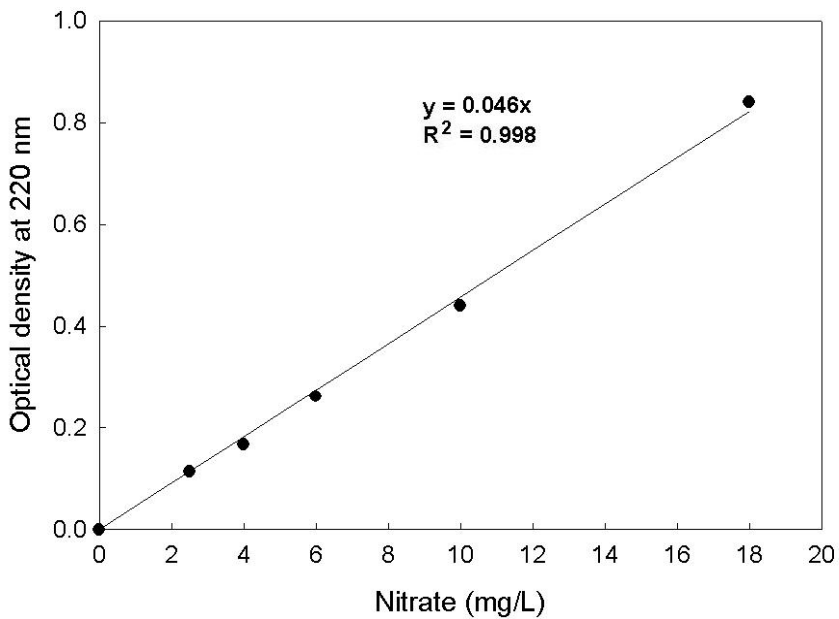


**Figure B- 2: Nitrate calibration**

## **Appendix C**

### **Concentration profile of growth nutrients in Fermentation 1**

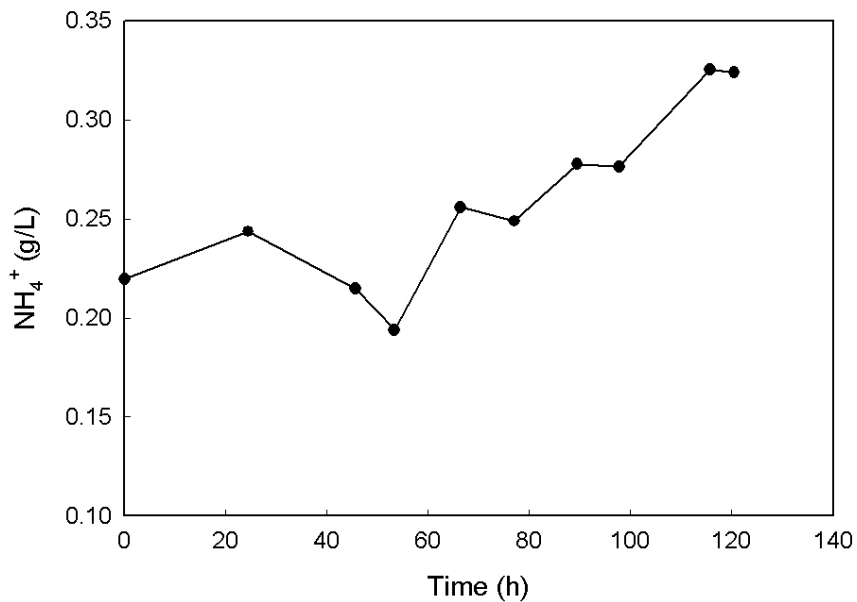


**Figure C- 1:** Ammonium concentration profile. Ammonium was fed semi-continuously for pH control.

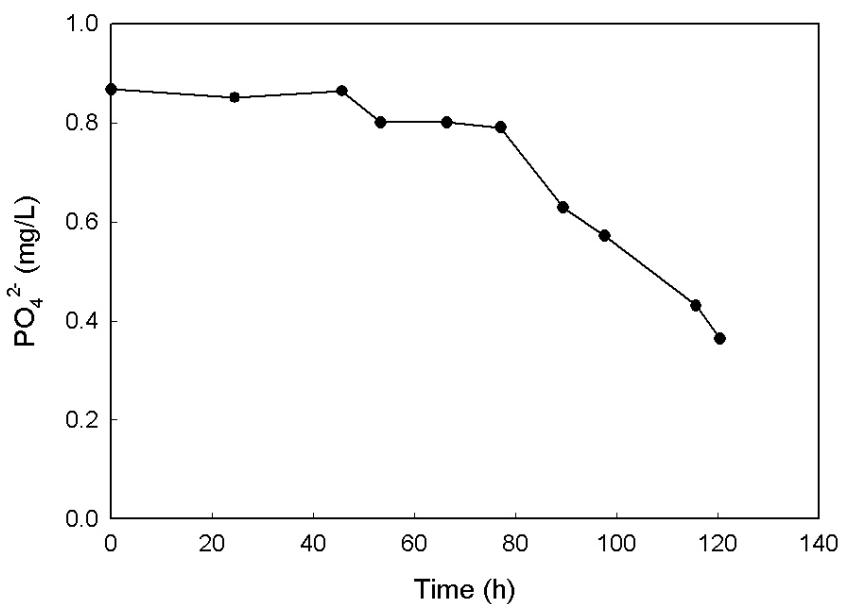


**Figure C- 2:** Phosphate concentration profile. No additional phosphate was fed.

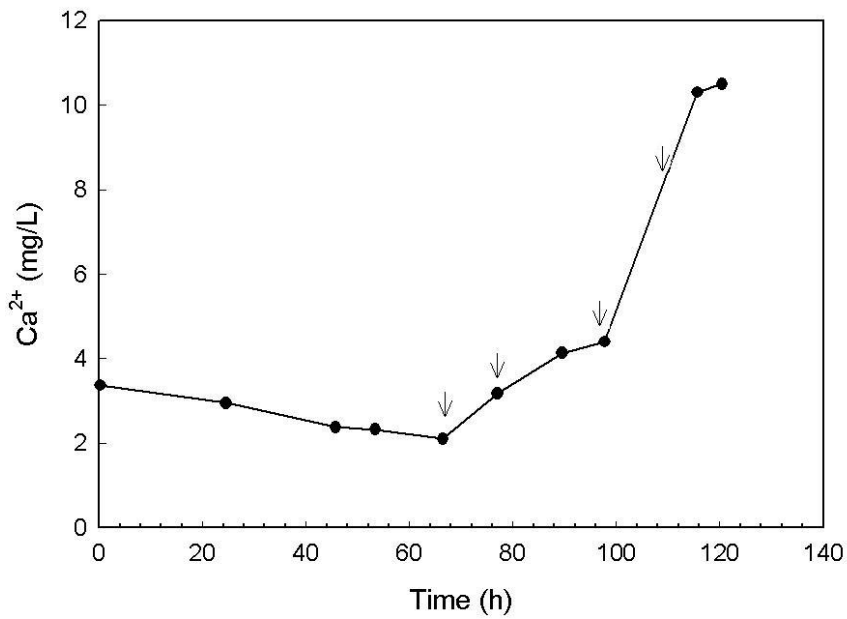


**Figure C- 3: Calcium concentration profile. Arrows indicate addition of 6.8 mg Ca<sup>2+</sup>.**

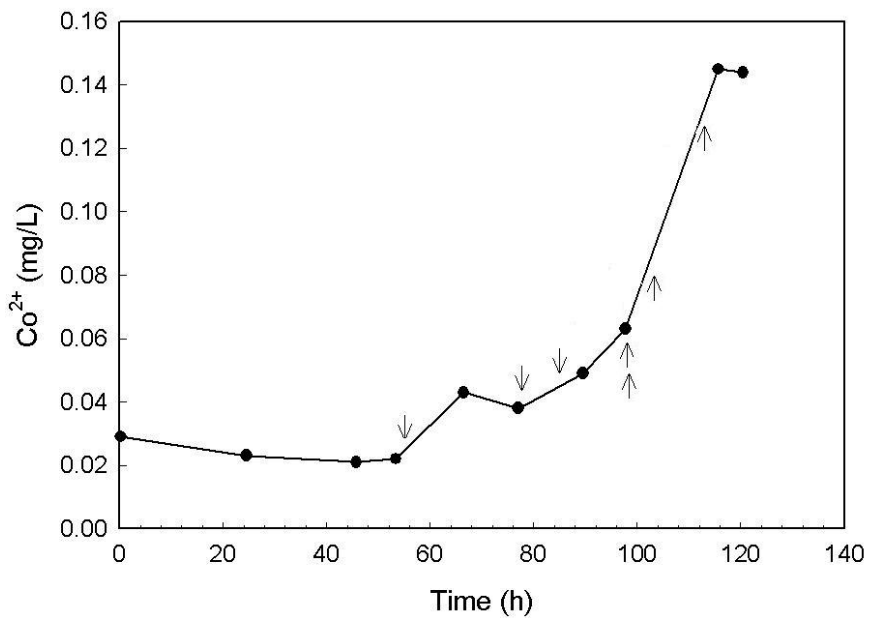


**Figure C- 4: Cobalt concentration profile. Arrows indicate addition of 0.08 mg cobalt.**

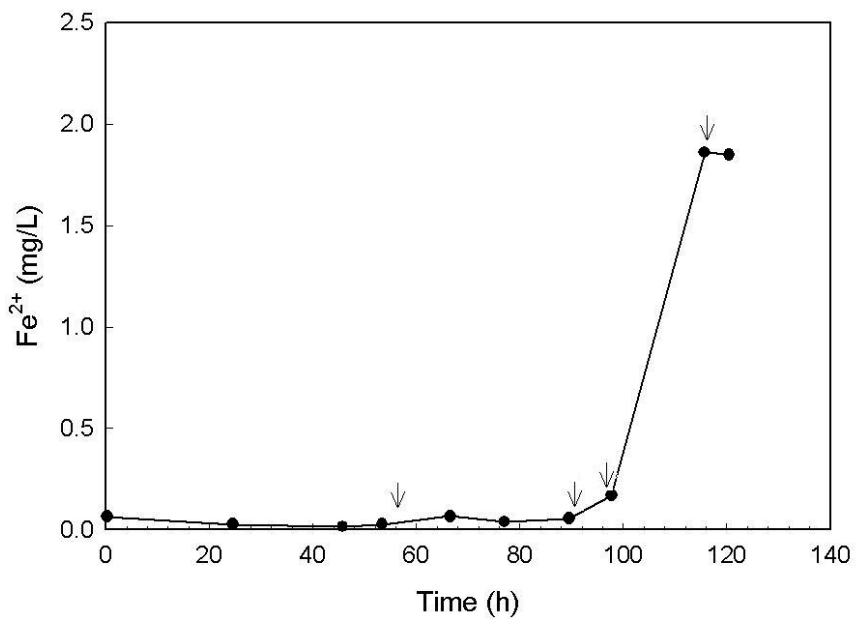


**Figure C- 5:** Iron concentration profile. Arrows indicate addition of 7.9 mg  $\text{Fe}^{2+}$ .

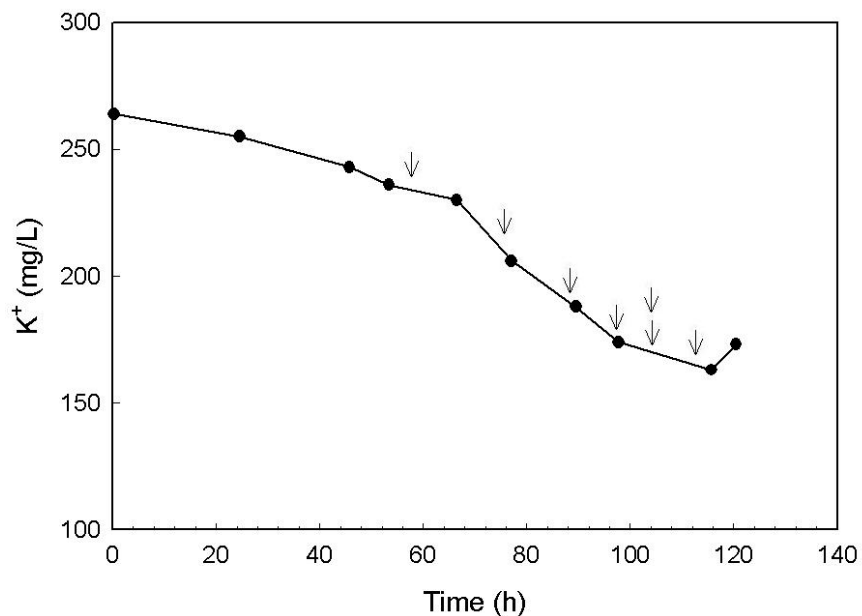


**Figure C- 6:** Potassium concentration profile. Arrows indicate addition of 0.13 mg potassium.

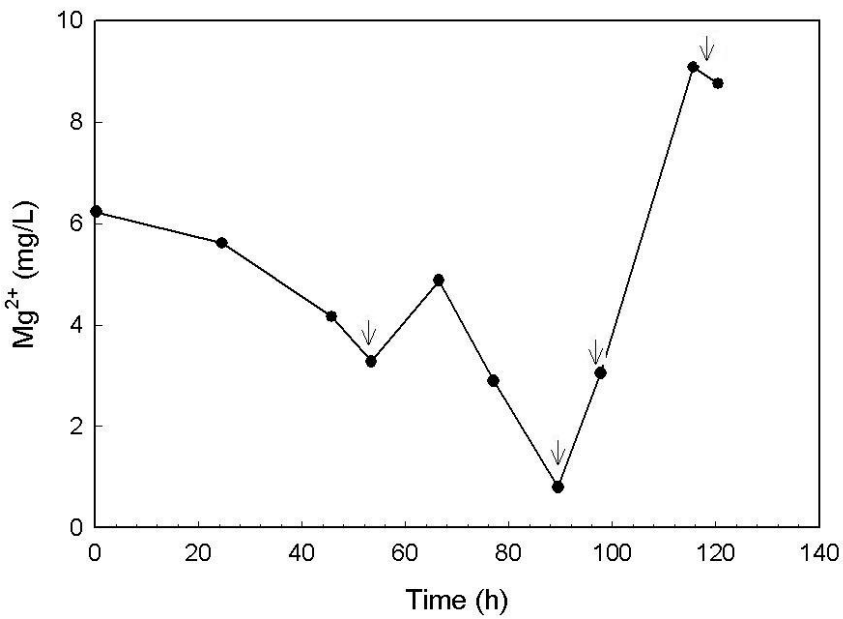


**Figure C- 7: Magnesium concentration profile. Arrows indicate addition of  $12.6\text{ mg }Mg^{2+}$ .**

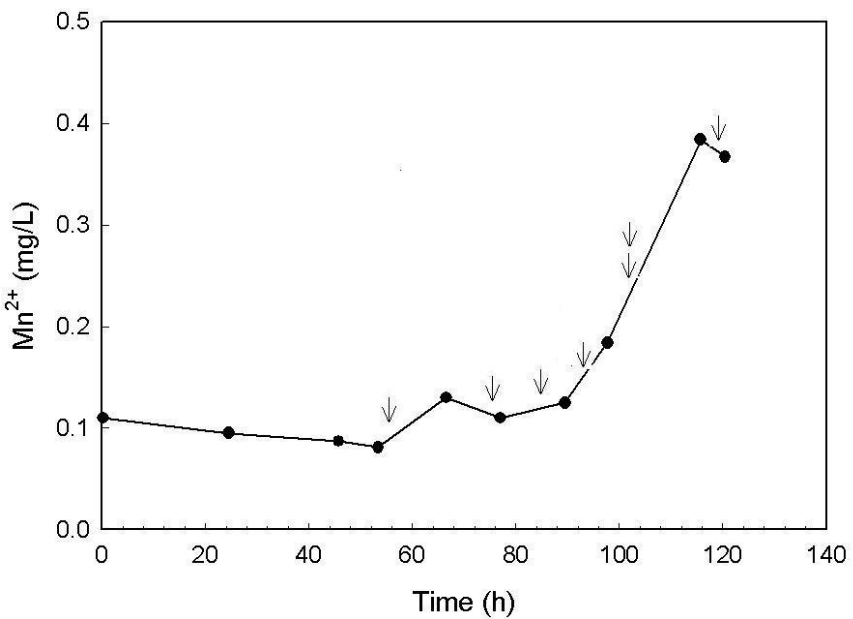


**Figure C- 8: Manganese concentration profile. Arrows indicate addition of  $0.3\text{ mg }Mn^{2+}$ .**

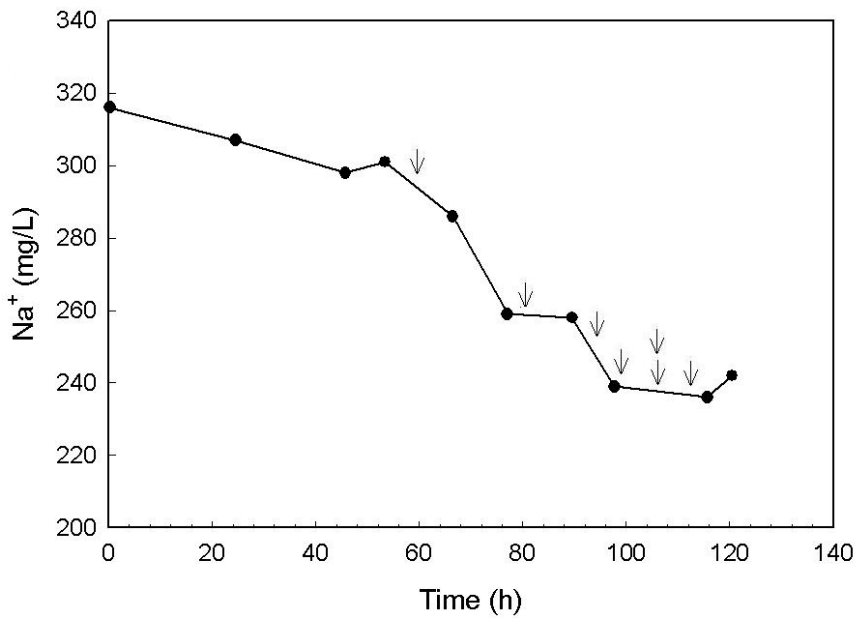


**Figure C- 9: Sodium concentration profile. Arrows indicate addition of 0.03 mg  $\text{Na}^+$ .**

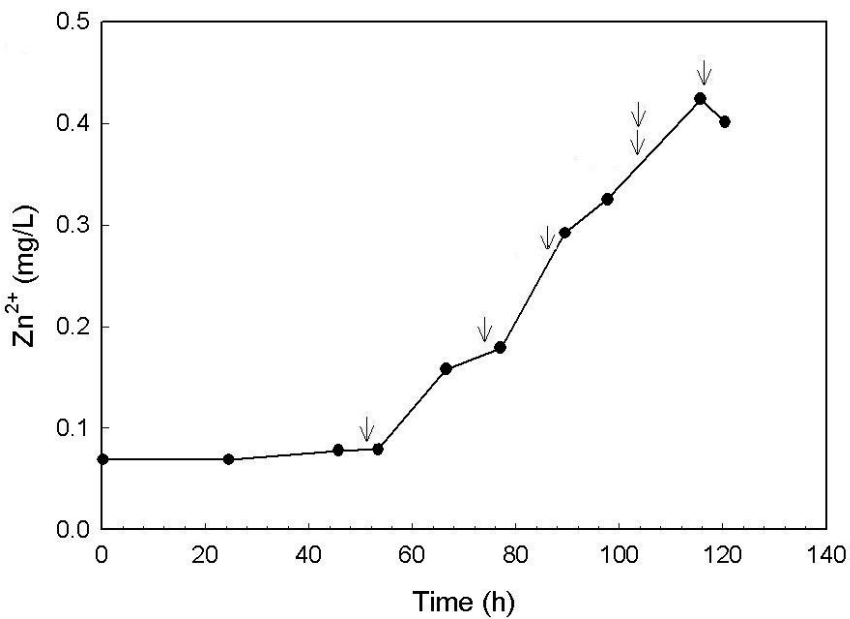


**Figure C- 10: Zinc concentration profile. Arrows indicate addition of 0.44 mg  $\text{Zn}^{2+}$ .**



## Appendix D

### Method for estimating specific growth rate in Fed-batch studies

Since there was no distinguishable lag phase observed during the fed-batch cultivation of *M. trichosporium OB3b*, a polynomial model was fit to the growth data to obtain a time relationship of biomass growth.

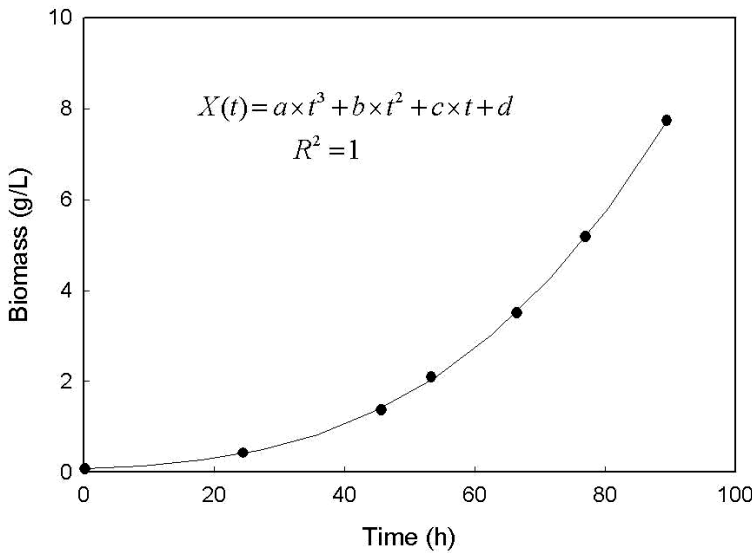
$$X(t) = a \times t^n + b \times t^{n-1} + \dots + c \times t^0 \quad \text{Equation D- 1}$$

Where X= biomass (g/L); t = time (h); n is the order of the polynomial; a,b,c are constants.

The specific growth rate,  $\mu$  was estimated by applying the following relationship.

$$\mu = \frac{1}{X} \frac{dX}{dt} \quad \text{Equation D- 2}$$

For example, in Fermentation 1, to estimate the specific growth rate at 53.38 h, a third order polynomial model was fit to the growth curve from 0 -89.95 h.



Where  $a = 8.57 \times 10^{-6}$ ;  $b = 1.29 \times 10^{-4}$ ;  $c = 5.41 \times 10^{-3}$  and  $d = 7.44 \times 10^{-2}$

At 53.38 h, the biomass measured was 2.1 g/L, hence the specific growth rate was determined with Equation D-2.

$$\mu = \frac{1}{X} \times \frac{dX}{dt} \Big|_{53.38\text{ h}} = 0.044 \text{ } (h^{-1})$$

## **Appendix E**

### **Biomass yield estimation**

Biomass yields from nutrients were determined from Fermentation 1 as the slope of the plot of the cumulative biomass (g) and cumulative substrate consumed (g or mg).

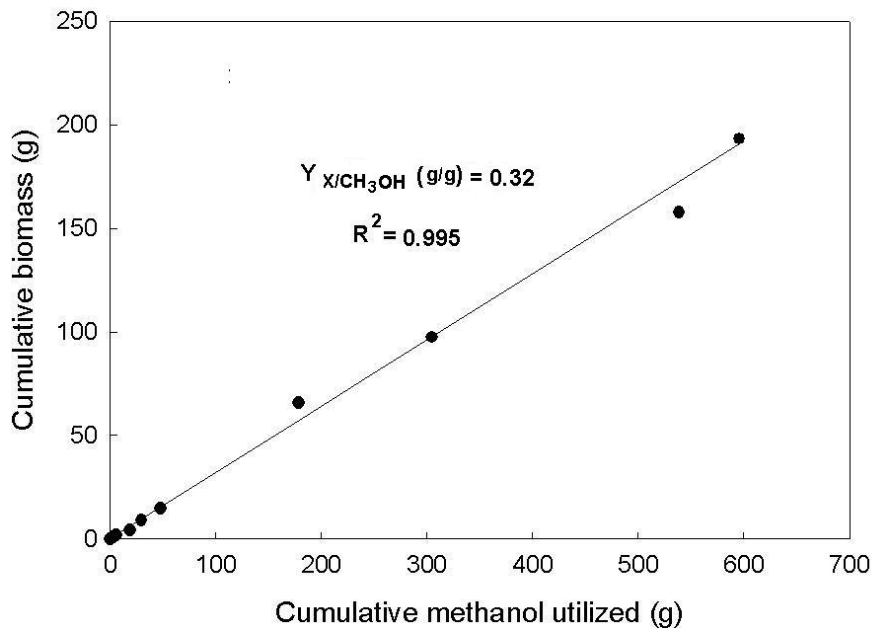


**Figure E- 1: Biomass yield on methanol**

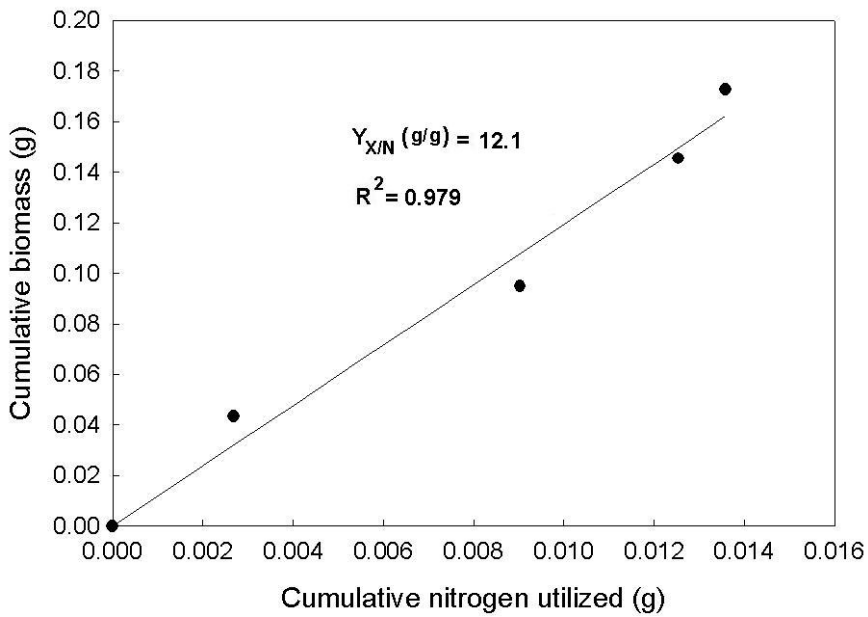


**Figure E- 2: Biomass yield on nitrogen (ammonium as nitrogen source)**

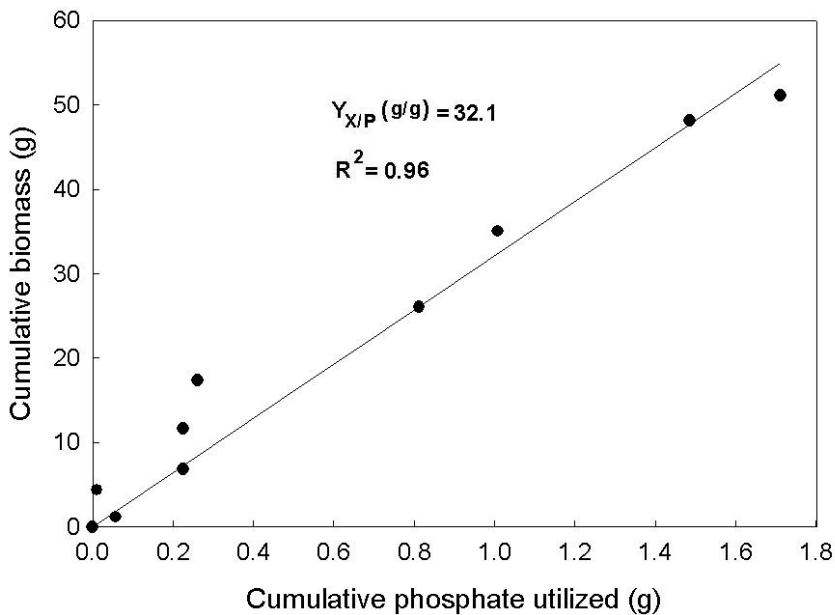


**Figure E- 3: Biomass yield on phosphate**

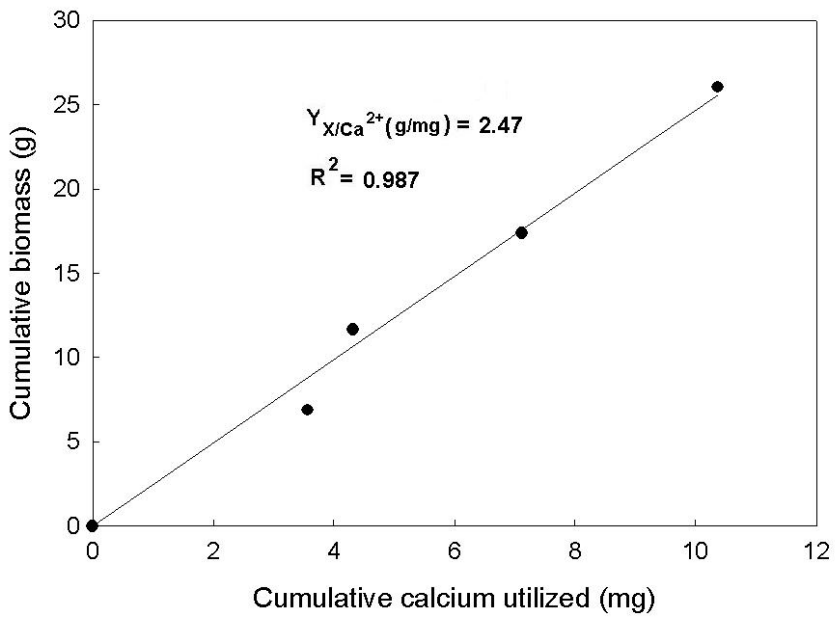


**Figure E- 4: Biomass yield on calcium**

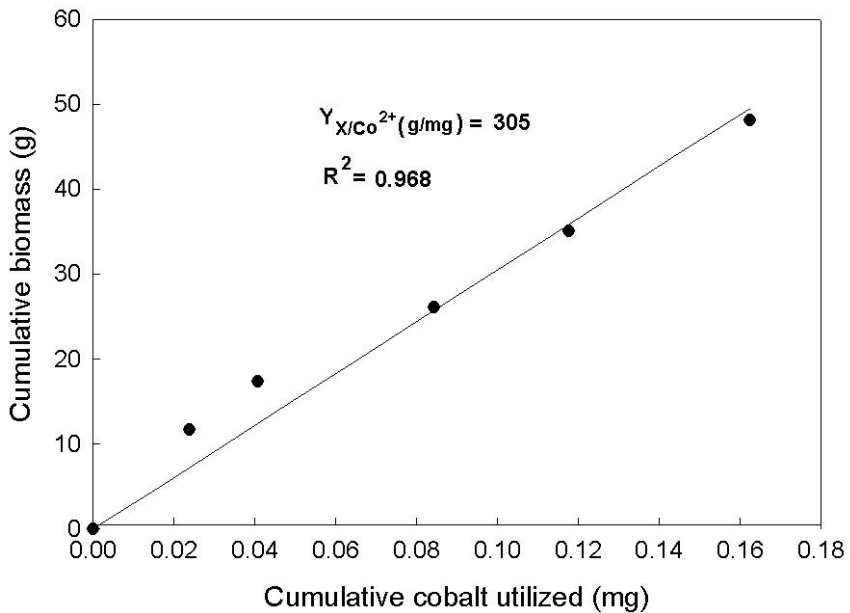


**Figure E- 5: Biomass yield on cobalt**

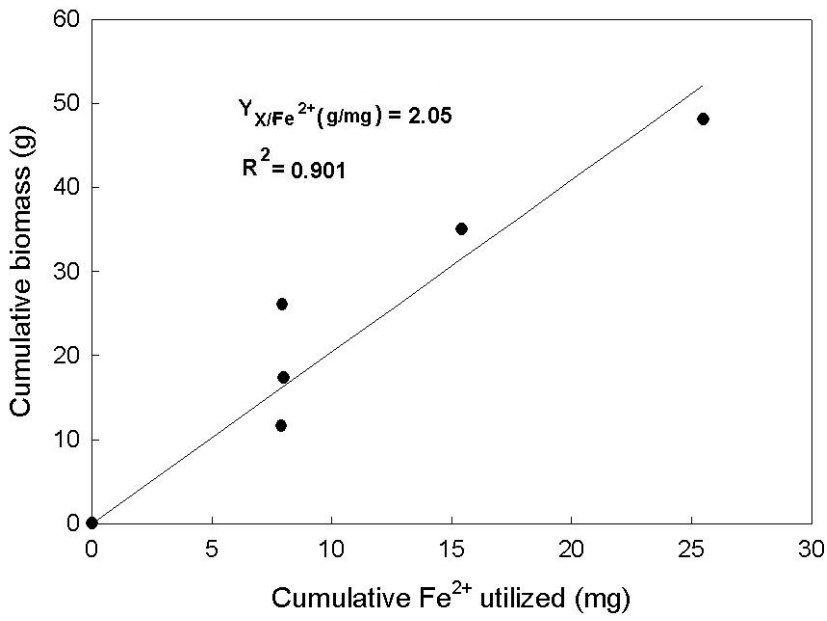


**Figure E- 6: Biomass yield on  $\text{Fe}^{2+}$**

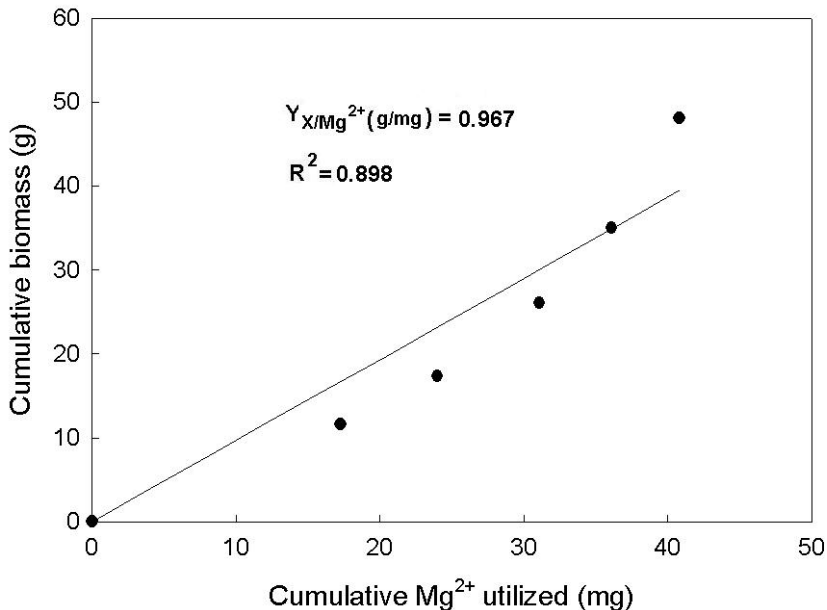


**Figure E- 7: Biomass yield on  $\text{Mg}^{2+}$**

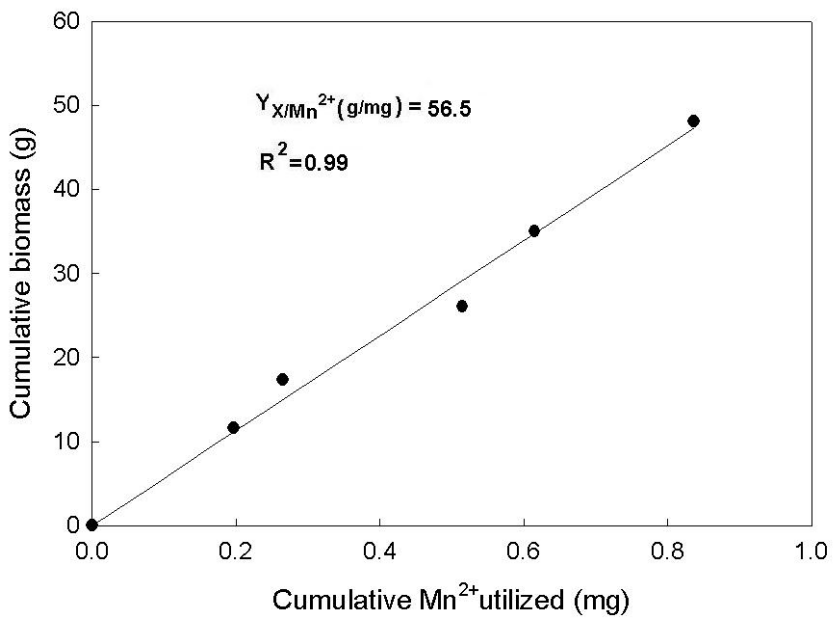


**Figure E- 8: Biomass yield on Mn<sup>2+</sup>**

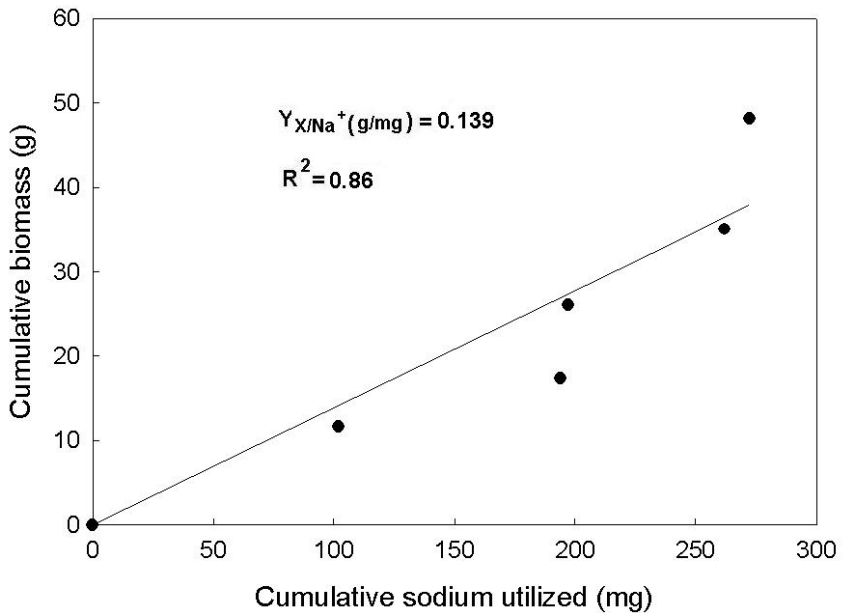


**Figure E- 9: Biomass yield on Na<sup>+</sup>**

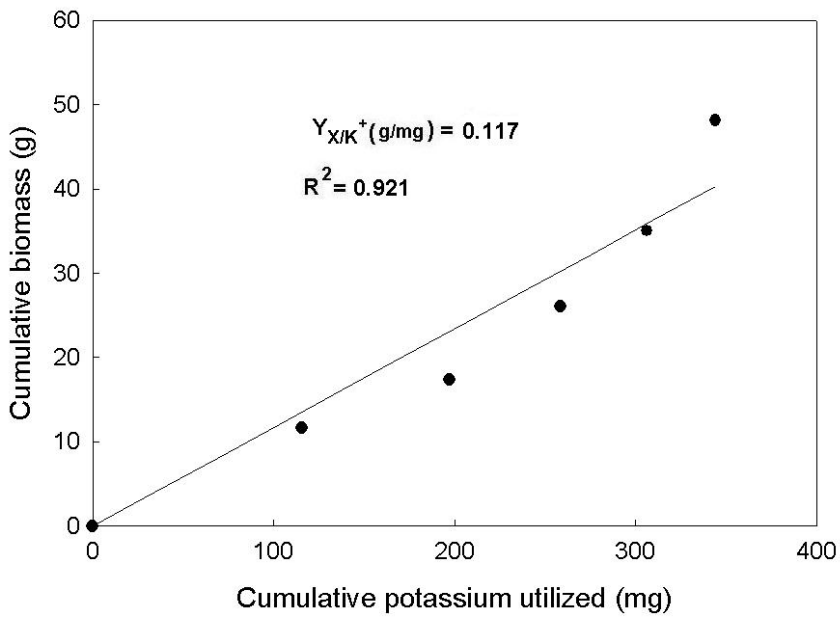


**Figure E- 10: Biomass yield on K<sup>+</sup>**

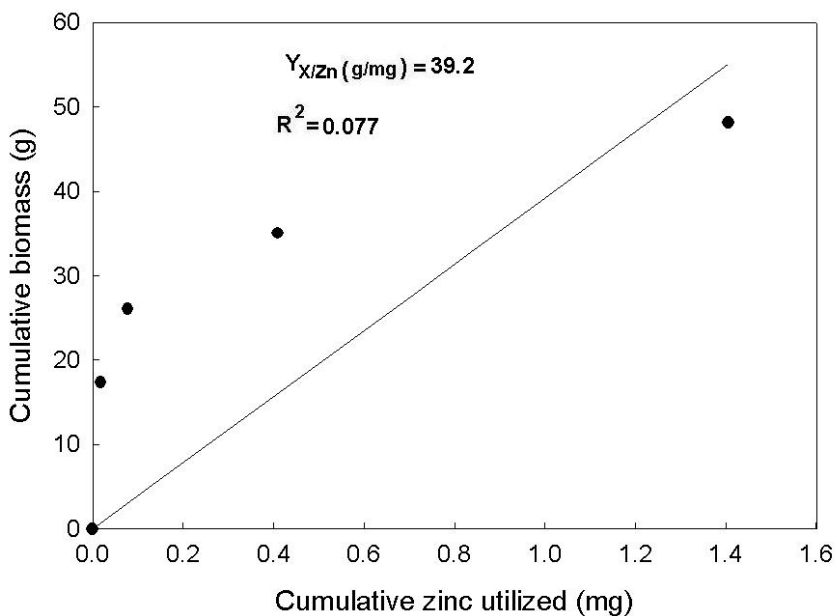


**Figure E- 11: Biomass yield on zinc**